Applied Mathematical Modelling 34 (2010) 1615–1633

Contents lists available at ScienceDirect

Applied Mathematical Modelling

journal homepage: www.elsevier.com/locate/apm

Treatment of singularities in the method of fundamental solutions for two-dimensional Helmholtz-type equations

Liviu Marin

Institute of Solid Mechanics, Romanian Academy, 15 Constantin Mille, Sector 1, P.O. Box 1-863, 010141 Bucharest, Romania

ARTICLE INFO

Article history:
Received 13 February 2009
Received in revised form 30 August 2009
Accepted 2 September 2009
Available online 11 September 2009

Keywords:
Helmholtz-type equations
Singular problems
Singularity subtraction technique (SST)
Method of fundamental solutions (MFS)

ABSTRACT

We investigate a meshless method for the accurate and non-oscillatory solution of problems associated with two-dimensional Helmholtz-type equations in the presence of boundary singularities. The governing equation and boundary conditions are approximated by the method of fundamental solutions (MFS). It is well known that the existence of boundary singularities affects adversely the accuracy and convergence of standard numerical methods. The solutions to such problems and/or their corresponding derivatives may have unbounded values in the vicinity of the singularity. This difficulty is overcome by subtracting from the original MFS solution the corresponding singular functions, without an appreciable increase in the computational effort and at the same time keeping the same MFS approximation. Four examples for both the Helmholtz and the modified Helmholtz equations are carefully investigated and the numerical results presented show an excellent performance of the approach developed.

1. Introduction

In many engineering problems governed by elliptic partial differential equations, boundary singularities arise when there are sharp re-entrant corners in the boundary, the boundary conditions change abruptly, or there are discontinuities in the material properties. It is well known that these situations give rise to singularities of various types and, as a consequence, the solutions to such problems and/or their corresponding derivatives may have unbounded values in the vicinity of the singularity. Singularities are known to affect adversely the accuracy and convergence of standard numerical methods, such as finite element (FEM), boundary element (BEM), finite-difference (FDM), spectral and meshless/meshfree methods. When the computed function is bounded, but has a branch point at the corner, the difficulty is not serious. Grid refinement and higher-order discretizations are common strategies aimed at improving the convergence rate and accuracy of the above-mentioned standard methods, see e.g. Apel et al. [1] or Apel and Nicaise [2]. If, however, the form of the singularity is taken into account and is properly incorporated into the numerical scheme then a more effective method may be constructed.

Helmholtz-type equations arise naturally in many physical applications related to wave propagation and vibration phenomena. They are often used to describe the vibration of a structure [3,4], the acoustic cavity problem [5,6], the radiation wave [7,8], the scattering of a wave [9,10] and the heat conduction in fins [11,12]. The knowledge of the associated boundary conditions on the entire boundary of the solution domain gives rise to problems for Helmholtz-type equations which have been extensively studied in the literature [13,14].

There are important studies regarding the numerical treatment of singularities occurring in Helmholtz-type equations. Time-harmonic waves in a membrane which contains one or more fixed edge stringers or cracks have been investigated by Chen et al. [4] who have employed the dual BEM in order to obtain an efficient solution of the Helmholtz equation in

E-mail addresses: marin.liviu@gmail.com, liviu@imsar.bu.edu.ro

0307-904X/$ - see front matter © 2009 Elsevier Inc. All rights reserved.
doi:10.1016/j.apm.2009.09.009

the presence of geometric singularities. Huang et al. [7] have investigated the electromagnetic field due to a line source radiating in the presence of a two-dimensional composite wedge made of a number of conducting and dielectric materials by employing the Fourier transform path integral method. A hybrid asymptotic/FEM for computing the acoustic field radiated or scattered by acoustically large objects has been developed by Barbone et al. [10]. Chen and Chen [15] have used the dual integral formulation for the Helmholtz equation to determine the acoustic modes of a two-dimensional cavity with a degenerate boundary. Schiff [16] has computed the transverse electric (TE) and transverse magnetic (TM) mode eigenvalues for ridged and other waveguides by using super-elements for the FEM, a refined local mesh and basis functions at the corner tip. The method of the auxiliary mapping, in conjunction with the *p*-version of the FEM, has been used by Cai et al. [17] and Lucas and Oh [18] in order to remove the pollution effect caused by singularities in the Helmholtz equation. Both Laplace and Helmholtz-type boundary value problems with singularities have been considered by Wu and Han [19], who have solved these problems using the FEM and by introducing a sequence of approximations to the boundary conditions at an artificial boundary and then reducing the original problems to boundary value problems away from the singularities. Xu and Chen [20] have used the FDM and higher-order discretized boundary conditions at the edges of perfectly conducting wedges for TE waves to retrieve accurately the field behaviour near a sharp edge. Mantič et al. [21] have recently investigated in a comprehensive way the singularity exponents and principal terms associated with multi-material corners in the case of anisotropic potential problems. The treatment of singularities in both isotropic and anisotropic two-dimensional Helmholtz-type equations has been addressed by Marin et al. [22], who have also modified the standard BEM to account for the presence of singularities. For an excellent survey on the treatment of singularities in elliptic boundary value problems, we refer the reader to Li and Lu [23] and the references therein.

The main idea in the method of fundamental solutions (MFS), which was originally introduced by Kupradze and Aleksidze [24] and numerically formulated for the first time by Mathon and Johnston [25], consists of approximating the solution of the problem by a linear combination of fundamental solutions with respect to some singularities/source points which are located outside the domain. Then the original problem is reduced to determining the unknown coefficients of the fundamental solutions and the coordinates of the source points by requiring the approximation to satisfy the boundary conditions and hence solving a nonlinear problem. If the source points are fixed *a priori* then the coefficients of the MFS approximation are determined by solving a linear problem. Excellent survey papers of the MFS and related methods over the past decades have been presented by Fairweather and Karageorghis [26], Golberg and Chen [27], Fairweather et al. [28] and Cho et al. [29].

The MFS has been successfully applied to solving a wide variety of boundary value problems. Karageorghis and Fairweather [30] have solved numerically the biharmonic equation using the MFS and later their method has been modified in order to take into account the presence of boundary singularities in both the Laplace and the biharmonic equations by Karageorghis [31] and Poullikkas et al. [32]. Furthermore, Poullikkas et al. [33] have investigated the numerical solution of the inhomogeneous harmonic and biharmonic equations by reducing these problems to the corresponding homogeneous cases and subtracting a particular solution of the governing equation. The application of the MFS to two-dimensional problems of steady-state heat conduction and elastostatics in isotropic and anisotropic bimaterials has been addressed by Berger and Karageorghis [34,35], whilst Poullikkas et al. [36] have successfully applied the MFS for solving three-dimensional elastostatics problems. Balakrishnan and Ramachandran [37] have employed the MFS for the numerical solution of linear diffusion reaction equations in irregular geometries in two and three dimensions. Karageorghis and Fairweather [38] have studied the use of the MFS for the approximate solution of three-dimensional isotropic materials with axisymmetrical geometry and both axisymmetrical and arbitrary boundary conditions. The MFS has been formulated for three-dimensional Signorini boundary value problems and it has been tested on a three-dimensional electropainting problem related to the coating of vehicle roofs in Poullikkas et al. [39]. The MFS, as well as another meshless method, namely the plane wave method, has been applied to acoustic wave scattering by Alves and Valtchev [40]. Young et al. [41] and Tsai et al. [42] have studied the application of the MFS to steady and unsteady Stokes problems, respectively. Recently, transient heat conduction problems have been approached via the MFS by Johansson and Lesnic [43].

The objective of this paper is to propose, implement and analyse a meshless method for the accurate and non-oscillatory solution of problems associated with two-dimensional Helmholtz-type equations in the presence of boundary singularities. In this study, the governing equation and corresponding boundary conditions are approximated by the MFS. The existence of boundary singularities affects adversely the accuracy and convergence of standard numerical methods. Consequently, the solutions to such problems and/or their corresponding derivatives, which are obtained by a straightforward inversion of the MFS system, may have unbounded values in the vicinity of the singularity. This difficulty is overcome by subtracting from the original MFS solution the corresponding singular functions, i.e. employing the so-called singularity subtraction technique (SST), without an appreciable increase in the computational effort and at the same time keeping the original MFS approximation. The proposed modified MFS is then implemented for problems associated with both the Helmholtz and the modified Helmholtz equations in two-dimensional domains with an edge crack or a V-notch, as well as an L-shaped domain.

2. Corner singularities for two-dimensional Helmholtz-type equations

In this section, some well-known results on the solution of the homogeneous two-dimensional Helmholtz-type equations are revised. For more details, we refer the reader to Marin et al. [22] and the references therein. For a fixed non-zero complex number $k = \alpha + i\beta$, where $\alpha, \beta \in \mathbb{R}$, the homogeneous Helmholtz-type equation in a two-dimensional domain $\Omega \subset \mathbb{R}^2$ reads as

$$\Delta u(\mathbf{x}) + k^2 u(\mathbf{x}) \equiv \frac{\partial^2 u(\mathbf{x})}{\partial x_1^2} + \frac{\partial^2 u(\mathbf{x})}{\partial x_2^2} + k^2 u(\mathbf{x}) = 0, \quad \mathbf{x} = (x_1, x_2) \in \Omega. \tag{1}$$

Let the polar coordinate system (r, θ) be defined in the usual way with respect to the Cartesian coordinates $(x_1, x_2) = (r\cos\theta, r\sin\theta)$. If we assume that the solution of Eq. (1) in the domain Ω can be written using the separation of variables with respect to the polar coordinates (r, θ), where $r > 0$, then the general solution of the Helmholtz-type equation (1) can be written as

$$u(r, \theta) = [\gamma_1 J_\lambda(kr) + \gamma_2 N_\lambda(kr)][a\cos(\lambda\theta) + b\sin(\lambda\theta)]. \tag{2}$$

Here γ_1, γ_2, a and b are constants, whilst J_λ and N_λ are the Bessel functions of the first kind and the second kind, respectively.

Consider now that Ω is a two-dimensional isotropic wedge domain of interior angle, $\theta_2 - \theta_1$, with the tip at the origin, O, of the local polar coordinates system and determined by two straight edges of angles θ_1 and θ_2, given by $\Omega = \{\mathbf{x} \in \mathbb{R}^2 | 0 < r < R(\theta), \theta_1 < \theta < \theta_2\}$, where $R(\theta)$ is either a bounded continuous function or infinity.

In the following, we consider the boundary value problem given by Eq. (1) in Ω and homogeneous Neumann and/or Dirichlet boundary conditions prescribed on the wedge edges. On assuming $Re\,\lambda \geqslant 0$ and taking into account the finite character of the solution, u, in a wedge tip neighbourhood, we obtain $\gamma_2 = 0$ in Eq. (2). Hence the basis function of singular functions to the aforementioned boundary value problem obtained from expression (2) can be written in the general form as

$$u^{(S)}(r, \theta) = J_\lambda(kr)[a\cos(\lambda\theta) + b\sin(\lambda\theta)], \tag{3}$$

where a and b are the unknown singular coefficients, whilst λ is referred to as the singularity exponent or eigenvalue. The singularity exponent/eigenvalue, as well as the corresponding singular coefficients, are determined by the geometry and boundary conditions along the boundaries sharing the singular point.

The normal flux through a straight radial line defined by an angle θ and associated with the normal vector $\mathbf{n}(\theta) = (-\sin\theta, \cos\theta)$ is given by

$$q^{(S)}(r, \theta) = \frac{1}{r}\frac{\partial}{\partial\theta} u^{(S)}(r, \theta). \tag{4}$$

For the sake of convenience, the singular function, $u^{(S)}$, and normal flux, $q^{(S)}$, given by equations (3) and (4), respectively, can be recast as:

$$u^{(S)}(r, \theta) = J_\lambda(kr)\{a\cos[\lambda(\theta - \theta_1)] + b\sin[\lambda(\theta - \theta_1)]\}, \tag{5}$$

$$q^{(S)}(r, \theta) = \frac{\lambda}{r} J_\lambda(kr)\{-a\sin[\lambda(\theta - \theta_1)] + b\cos[\lambda(\theta - \theta_1)]\}. \tag{6}$$

In this study, four configurations of homogeneous Neumann (N) and Dirichlet (D) boundary conditions at the wedge edges applied to expressions (5) and (6) are considered. The conditions which allow a nontrivial solution of the resulting system of equations under the assumption $Re\,\lambda \geqslant 0$ are listed below:

Case I: N–N wedge

$$q^{(S)}(r, \theta_1) = q^{(S)}(r, \theta_2) = 0 \;\Rightarrow\; b = 0 \text{ and } \sin[\lambda(\theta_2 - \theta_1)] = 0 \;\Rightarrow\; \lambda = n\frac{\pi}{\theta_2 - \theta_1},\ n \geqslant 0 \tag{7}$$

Case II: D–D wedge

$$u^{(S)}(r, \theta_1) = u^{(S)}(r, \theta_2) = 0 \;\Rightarrow\; a = 0 \text{ and } \sin[\lambda(\theta_2 - \theta_1)] = 0 \;\Rightarrow\; \lambda = n\frac{\pi}{\theta_2 - \theta_1},\ n \geqslant 1 \tag{8}$$

Case III: N–D wedge

$$q^{(S)}(r, \theta_1) = u^{(S)}(r, \theta_2) = 0 \;\Rightarrow\; b = 0 \text{ and } \cos[\lambda(\theta_2 - \theta_1)] = 0 \;\Rightarrow\; \lambda = \left(n - \frac{1}{2}\right)\frac{\pi}{\theta_2 - \theta_1},\ n \geqslant 1 \tag{9}$$

Case IV: D–N wedge

$$u^{(S)}(r, \theta_1) = q^{(S)}(r, \theta_2) = 0 \;\Rightarrow\; a = 0 \text{ and } \cos[\lambda(\theta_2 - \theta_1)] = 0 \;\Rightarrow\; \lambda = \left(n - \frac{1}{2}\right)\frac{\pi}{\theta_2 - \theta_1},\ n \geqslant 1 \tag{10}$$

From formulae (7)–(10) it can be noticed that the singularity exponents, λ, are real and simple and they coincide in cases I and II, and III and IV, respectively. Using the above results, the general asymptotic expansions for the singular function of Helmholtz-type equations for a single wedge and corresponding to homogeneous Neumann and Dirichlet boundary conditions on the wedge edges are obtained in the following form:

Case I: N–N wedge

$$u^{(S)}(r, \theta) = \sum_{n=0}^{\infty} a_n u_n^{(NN)}(r, \theta) = \sum_{n=0}^{\infty} a_n J_{\lambda_n}(kr)\cos[\lambda_n(\theta - \theta_1)], \quad \lambda_n = n\frac{\pi}{\theta_2 - \theta_1},\ n \geqslant 0 \tag{11}$$

Case II: D–D wedge

$$u^{(S)}(r,\theta)=\sum_{n=1}^{\infty}a_n u_n^{(DD)}(r,\theta)=\sum_{n=0}^{\infty}a_n J_{\lambda_n}(kr)\,\sin[\lambda_n(\theta-\theta_1)],\quad \lambda_n=n\frac{\pi}{\theta_2-\theta_1},\ n\geqslant 1 \tag{12}$$

Case III: N–D wedge

$$u^{(S)}(r,\theta)=\sum_{n=1}^{\infty}a_n u_n^{(ND)}(r,\theta)=\sum_{n=0}^{\infty}a_n J_{\lambda_n}(kr)\,\cos[\lambda_n(\theta-\theta_1)],\quad \lambda_n=\left(n-\frac{1}{2}\right)\frac{\pi}{\theta_2-\theta_1},\ n\geqslant 1 \tag{13}$$

Case IV: D–N wedge

$$u^{(S)}(r,\theta)=\sum_{n=1}^{\infty}a_n u_n^{(DN)}(r,\theta)=\sum_{n=0}^{\infty}a_n J_{\lambda_n}(kr)\,\sin[\lambda_n(\theta-\theta_1)],\quad \lambda_n=\left(n-\frac{1}{2}\right)\frac{\pi}{\theta_2-\theta_1},\ n\geqslant 1 \tag{14}$$

3. Singularity subtraction technique

Consider a two-dimensional bounded domain Ω with a piecewise smooth boundary $\Gamma=\partial\Omega$ which contains a singularity at the point $O(\mathbf{x}^0)$, $\mathbf{x}^0=(x_1^0,x_2^0)$, that may be caused by a change in the boundary conditions at the origin and/or a re-entrant corner at the origin. For the simplicity of the following explanations, it is assumed that the singularity point is located at the intersection of the Dirichlet and Neumann boundary parts, see e.g. Fig. 1d, although the method presented herein can easily be extended to other local configurations or boundary conditions. Hence the problem to be solved recasts as

$$\Delta u(\mathbf{x})+k^2u(\mathbf{x})=0,\quad \mathbf{x}\in\Omega \tag{15.1}$$
$$u(\mathbf{x})=\tilde{u}(\mathbf{x}),\quad \mathbf{x}\in\Gamma_{\mathrm{D}} \tag{15.2}$$
$$q(\mathbf{x})\equiv\nabla u(\mathbf{x})\cdot\mathbf{n}(\mathbf{x})=\tilde{q}(\mathbf{x}),\quad \mathbf{x}\in\Gamma_{\mathrm{N}} \tag{15.3}$$

where $\Gamma_{\mathrm{D}},\Gamma_{\mathrm{N}}\neq\emptyset$, $\overline{\Gamma}_{\mathrm{D}}\cup\overline{\Gamma}_{\mathrm{N}}=\Gamma$, $\Gamma_{\mathrm{D}}\cap\Gamma_{\mathrm{N}}=\emptyset$, $\{O\}\subset\overline{\Gamma}_{\mathrm{D}}\cap\overline{\Gamma}_{\mathrm{N}}$, $\tilde{u}$ and $\tilde{q}$ are prescribed boundary solution and normal flux, respectively, and we denote the closure of a set by an overbar.

In order to avoid numerical difficulties arising from the presence of the singularity in the solution at O it is convenient to modify the original problem before it is solved by the MFS. Due to the linearity of the Helmholtz and modified Helmholtz operators, as well as the boundary conditions, the superposition principle is valid and the solution, u, and the normal flux, q, can be written as

$$u(\mathbf{x})=\left(u(\mathbf{x})-u^{(S)}(\mathbf{x})\right)+u^{(S)}(\mathbf{x})=u^{(R)}(\mathbf{x})+u^{(S)}(\mathbf{x}),\quad \mathbf{x}\in\overline{\Omega}=\Omega\cup\Gamma, \tag{16}$$
$$q(\mathbf{x})=\left(q(\mathbf{x})-q^{(S)}(\mathbf{x})\right)+q^{(S)}(\mathbf{x})=q^{(R)}(\mathbf{x})+q^{(S)}(\mathbf{x}),\quad \mathbf{x}\in\Gamma, \tag{17}$$

where $u^{(S)}(\mathbf{x})$ is a particular singular solution which satisfies Eq. (15.1) and the corresponding homogeneous boundary conditions on the parts of the boundary containing the singularity point O and $q^{(S)}(\mathbf{x})\equiv\nabla u^{(S)}(\mathbf{x})\cdot\mathbf{n}(\mathbf{x})$ is its conormal derivative. If appropriate functions are chosen for the singular solution and its conormal derivative then the numerical analysis can be carried out for the regular solution $u^{(R)}(\mathbf{x})$ and its conormal derivative $q^{(R)}(\mathbf{x})\equiv\nabla u^{(R)}(\mathbf{x})\cdot\mathbf{n}(\mathbf{x})$ only. In terms of the regular solution $u^{(R)}(\mathbf{x})$, the original problem (15.1)–(15.3) becomes

$$\Delta u^{(R)}(\mathbf{x})+k^2u^{(R)}(\mathbf{x})=0,\quad \mathbf{x}\in\Omega \tag{18.1}$$
$$u^{(R)}(\mathbf{x})=\tilde{u}(\mathbf{x})-u^{(S)}(\mathbf{x}),\quad \mathbf{x}\in\Gamma_{\mathrm{D}} \tag{18.2}$$
$$q^{(R)}(\mathbf{x})=\tilde{q}(\mathbf{x})-q^{(S)}(\mathbf{x}),\quad \mathbf{x}\in\Gamma_{\mathrm{N}} \tag{18.3}$$

The modified boundary conditions (18.2) and (18.3) introduce additional unknowns into the problem, which are the constants of the particular solution used to represent the singular function. It should be noted that these constants are similar to the stress intensity factors corresponding to an analogous problem for the Lamé system and, in what follows, they will be referred to as "flux intensity factors". Since the flux intensity factors are unknown at this stage of the problem, they become primary unknowns.

In order to obtain a unique solution to the regular problem (18.1)–(18.3), it is necessary to specify additional constraints which must be as many as the number of the unknown flux intensity factors, i.e. one for each singular function/eigenfunction included in the analysis. These extra conditions must be applied in such a way that the cancelation of the singularity in the regular solution is ensured. This is achieved by constraining the regular solution and/or its conormal derivative directly in a neighbourhood of the singularity point O

$$u^{(R)}(\mathbf{x})=0,\ \mathbf{x}\in\Gamma_{\mathrm{N}}\cap B(O;\tau)\quad \text{and/or}\quad q^{(R)}(\mathbf{x})=0,\ \mathbf{x}\in\Gamma_{\mathrm{D}}\cap B(O;\tau), \tag{19}$$

where $B(O;\tau)=\{\mathbf{x}\in\mathbb{R}^2\,|\,\|\mathbf{x}-\mathbf{x}^0\|<\tau\}$, $\tau>0$ is sufficiently small and $\|\cdot\|$ represents the Euclidean norm.

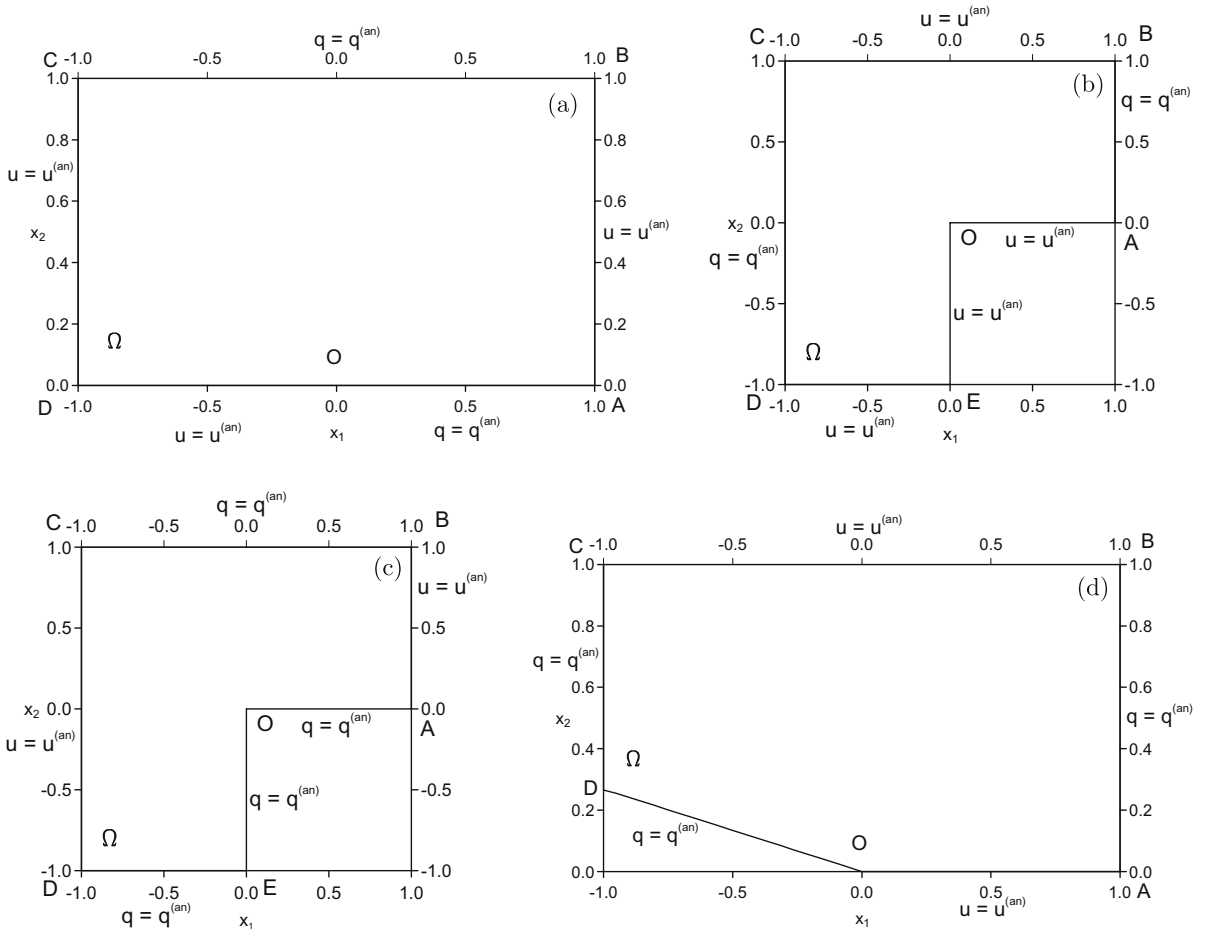

Fig. 1. Schematic diagram of the geometry and boundary conditions for the singular problems investigated, namely (a) Example 1: N–D singular problem in a domain containing an edge crack OD with $\theta_1 = 0$ and $\theta_2 = \pi$; (b) Example 2: D–D singular problem in an L-shaped domain with $\theta_1 = 0$ and $\theta_2 = 3\pi/2$; (c) Example 3: N–N singular problem in an L-shaped domain with $\theta_1 = 0$ and $\theta_2 = 3\pi/2$; and (d) Example 4: D–N singular inverse problem in a domain containing a V-notch with $\theta_1 = 0$ and $\theta_2 = 11\pi/12$.

4. The method of fundamental solutions

The fundamental solutions $\mathscr{F}_H$ and $\mathscr{F}_{MH}$ of the Helmholtz $(k = \alpha + i\beta, \alpha \in \mathbb{R}, \beta = 0)$ and modified Helmholtz $(k = \alpha + i\beta, \alpha = 0, \beta \in \mathbb{R})$ equations, respectively, in the two-dimensional case are given by, see e.g. Fairweather and Karageorghis [26],

$$\mathscr{F}_H(\mathbf{x},\mathbf{y}) = \frac{i}{4} H_0^{(1)}(k\|\mathbf{x}-\mathbf{y}\|), \quad \mathbf{x} \in \overline{\Omega}, \quad \mathbf{y} \in \mathbb{R}^2 \setminus \overline{\Omega}, \tag{20}$$

and

$$\mathscr{F}_{MH}(\mathbf{x},\mathbf{y}) = \frac{1}{2\pi} K_0(k\|\mathbf{x}-\mathbf{y}\|), \quad \mathbf{x} \in \overline{\Omega}, \quad \mathbf{y} \in \mathbb{R}^2 \setminus \overline{\Omega}, \tag{21}$$

respectively. Here $\mathbf{x} = (x_1, x_2)$ is either a boundary or a domain point, $\mathbf{y} = (y_1, y_2)$ is a source point, $H_0^{(1)}$ is the Hankel function of the first kind of order zero and K_0 is the modified Bessel function of the second kind of order zero.

According to the MFS approach, the regular solution, $u^{(R)}$, in the solution domain is approximated by a linear combination of fundamental solutions with respect to M source points $\mathbf{y}^m$ in the form

$$u^{(R)}(\mathbf{x}) \approx \sum_{m=1}^{M} c_m \mathscr{F}(\mathbf{x},\mathbf{y}^m), \quad \mathbf{x} \in \overline{\Omega}, \tag{22}$$

where $\mathscr{F} = \mathscr{F}_H$ in the case of the Helmholtz equation, $\mathscr{F} = \mathscr{F}_{MH}$ in the case of the modified Helmholtz equation, $c_m \in \mathbb{R}$, $m = 1, \ldots, M$, are the unknown coefficients. Then the regular normal flux on the boundary Γ can be approximated by

$$q^{(\mathrm{R})}(\mathbf{x}) \approx \sum_{m=1}^{M} c_m \mathscr{G}(\mathbf{x}, \mathbf{y}^m), \quad \mathbf{x} \in \Gamma, \tag{23}$$

where $\mathscr{G}(\mathbf{x}, \mathbf{y}) \equiv \nabla_{\mathbf{x}} \mathscr{F}(\mathbf{x}, \mathbf{y}) \cdot \mathbf{n}(\mathbf{x})$, while $\mathscr{G} = \mathscr{G}_H$ in the case of the Helmholtz equation and $\mathscr{G} = \mathscr{G}_{MH}$ in the case of the modified Helmholtz equation are given by

$$\mathscr{G}_H(\mathbf{x}, \mathbf{y}) = -\frac{[(\mathbf{x}-\mathbf{y}) \cdot \mathbf{n}(\mathbf{x})] k i}{4 \|\mathbf{x}-\mathbf{y}\|} H_1^{(1)}(k\|\mathbf{x}-\mathbf{y}\|), \quad \mathbf{x} \in \Gamma, \quad \mathbf{y} \in \mathbb{R}^2 \setminus \overline{\Omega}, \tag{24}$$

and

$$\mathscr{G}_{MH}(\mathbf{x}, \mathbf{y}) = -\frac{[(\mathbf{x}-\mathbf{y}) \cdot \mathbf{n}(\mathbf{x})] k}{2\pi \|\mathbf{x}-\mathbf{y}\|} K_1(k\|\mathbf{x}-\mathbf{y}\|), \quad \mathbf{x} \in \Gamma, \quad \mathbf{y} \in \mathbb{R}^2 \setminus \overline{\Omega}, \tag{25}$$

respectively. Here $H_1^{(1)}$ is the Hankel function of the first kind of order one and K_1 is the modified Bessel function of the second kind of order one.

If the solution domain is a disk of radius r, it was shown in [44,45] that, when the collocation and source points are placed uniformly on the boundary of the disk and on a circle of radius R, $R > r$, respectively, then the error in the MFS approximation for L collocation points and L singularities satisfies $\sup_{\mathbf{x} \in \Omega} = O((r/R)^L)$, i.e. exponential convergence is achieved. Furthermore, this result was generalised to two-dimensional regions whose boundaries are analytic Jordan curves by Katsurada [46,47]. It is worth mentioning that the functional approximation given by Eq. (22) is also consistent, in the sense that this functional also approximates accurately the exact solution of the problem not only on the boundary Γ, but also in the interior of the solution domain Ω, see Kondepalli et al. [48] and MacDonell [49]. Moreover, the MFS approximation (22) is capable of reproducing various types of solutions to Helmholtz-type equations, such as constant, linear, quadratic, exponential, trigonometric functions, etc., see e.g. Fairweather and Karageorghis [26] and Golberg and Chen [27].

Assume that the singular point O is located between the collocation points $\mathbf{x}^{n_{\mathrm{D}}^0} \in \Gamma_{\mathrm{D}}$ and $\mathbf{x}^{n_{\mathrm{N}}^0} \in \Gamma_{\mathrm{N}}$, and n_{S} singular functions/eigenfunctions $u_n^{(\mathrm{DN})}(r, \theta)$, as well as flux intensities, a_n, are taken into account, such that the additional constraints for the regular solution and/or its conormal derivative given by Eq. (19) read as

$$u^{(\mathrm{R})}(\mathbf{x}^{n_{\mathrm{N}}^0+1-m}) = 0 \quad \text{for} \quad 2m-1 \in \{1, \ldots, n_{\mathrm{S}}\}, \tag{26}$$

and

$$q^{(\mathrm{R})}(\mathbf{x}^{n_{\mathrm{D}}^0-1+m}) = 0 \quad \text{for} \quad 2m \in \{1, \ldots, n_{\mathrm{S}}\}. \tag{27}$$

If n_{D} collocation points $\mathbf{x}^{\ell}$, $\ell = 1, \ldots, n_{\mathrm{D}}$, and n_{N} collocation points $\mathbf{x}^{n_{\mathrm{D}}+\ell}$, $\ell = 1, \ldots, n_{\mathrm{N}}$, are chosen on the boundaries Γ_{D} and Γ_{N}, respectively, such that $L = n_{\mathrm{D}} + n_{\mathrm{N}}$, and the location of the source points $\mathbf{y}^m$, $m = 1, \ldots, M$, is set then the boundary value problem (18.1)–(18.3), together with the additional conditions (19), recasts as a system of $(L + n_{\mathrm{S}})$ linear algebraic equations with $(M + n_{\mathrm{S}})$ unknowns which can be generically written as

$$\mathbf{A}\tilde{\mathbf{c}} = \mathbf{F}, \tag{28}$$

where $\tilde{\mathbf{c}} = (c_1, \ldots, c_M, \alpha_1, \ldots, \alpha_{n_{\mathrm{S}}}) \in \mathbb{R}^{M+n_{\mathrm{S}}}$ and the components of the MFS matrix

$\mathbf{A} \in \mathbb{R}^{(L+n_{\mathrm{S}}) \times (M+n_{\mathrm{S}})}$ and right-hand side vector $\mathbf{F} \in \mathbb{R}^{L+n_{\mathrm{S}}}$ are given by

$$A_{ij} = \begin{cases} \mathscr{F}(\mathbf{x}^{\ell}, \mathbf{y}^m), & \ell = 1, \ldots, n_{\mathrm{D}}, & m = 1, \ldots, M \\ u_{m-M}^{(\mathrm{DN})}(r^{\ell}, \theta^{\ell}), & \ell = 1, \ldots, n_{\mathrm{D}}, & m = M+1, \ldots, \mathrm{M}+n_{\mathrm{S}} \\ \mathscr{G}(\mathbf{x}^{\ell}, \mathbf{y}^m), & \ell = n_{\mathrm{D}}+1, \ldots, n_{\mathrm{D}}+n_{\mathrm{N}}, & m = 1, \ldots, M \\ q_{m-M}^{(\mathrm{DN})}(r^{\ell}, \theta^{\ell}), & \ell = n_{\mathrm{D}}+1, \ldots, n_{\mathrm{D}}+n_{\mathrm{N}}, & m = M+1, \ldots, M+n_{\mathrm{S}} \\ \mathscr{F}(\mathbf{x}^{n_{\mathrm{N}}^0+1-m-N}, \mathbf{y}^m), & \ell - \mathrm{L} = 2m-1 \in \{1, \ldots, n_{\mathrm{S}}\}, & \mathrm{m} = 1, \ldots, M \\ \mathscr{G}(\mathbf{x}^{n_{\mathrm{D}}^0-1+m-N}, \mathbf{y}^m), & \ell - \mathrm{L} = 2m \in \{1, \ldots, n_{\mathrm{S}}\}, & \mathrm{m} = 1, \ldots, M \\ 0, & \ell - L \in \{1, \ldots, n_{\mathrm{S}}\}, & m = M+1, \ldots, M+n_{\mathrm{S}} \end{cases} \tag{29}$$

$$F_{\ell} = \begin{cases} \tilde{u}(\mathbf{x}^{\ell}), & \ell = 1, \ldots, n_{\mathrm{D}} \\ \tilde{q}(\mathbf{x}^{\ell}), & \ell = n_{\mathrm{D}}+1, \ldots, n_{\mathrm{D}}+n_{\mathrm{N}} \\ 0, & \ell = n_{\mathrm{D}}+n_{\mathrm{N}}+1, \ldots, n_{\mathrm{D}}+n_{\mathrm{N}}+n_{\mathrm{S}} \end{cases} \tag{30}$$

Here $(r^{\ell}, \theta^{\ell})$ are the local polar coordinates of the collocation point $\mathbf{x}^{\ell}$, $\ell = 1, \ldots, L$.

It should be noted that in order to uniquely determine the solution $\tilde{\mathbf{c}}$ of the system of linear algebraic equations (28), i.e. the coefficients c_m, $m = 1, \ldots, M$, in approximations (22) and (23), and the flux intensity factors a_n, $n = 1, \ldots, n_{\mathrm{S}}$, in the asymptotic expansions (11)–(14), the total number of collocation points corresponding to the Dirichlet and Neumann boundary conditions, L, and the number of source points, M, must satisfy the inequality $M \leqslant L$. It is important to mention that the complex MFS + SST system (28) resulting in the case of the Helmholtz equation has been solved by equating both its real and imaginary parts.

In order to implement the MFS, the location of the source points has to be determined and this is usually achieved by considering either the static or the dynamic approach. In the static approach, the source points are pre-assigned and kept fixed throughout the solution process, this approach reducing to solving a linear problem [26]. In the dynamic approach, the source points and the unknown coefficients are determined simultaneously during the solution process via a system of nonlinear equations which may be solved using minimization methods [26]. Therefore, we have decided to employ the static approach in our computations with the source points located on a so-called pseudo-boundary which has the same shape as the boundary of the domain [50].

5. Numerical results and discussion

It is the purpose of this section to present the performance of the modified MFS described in Section 4. To do so, we solve numerically the direct boundary value problem (15.1)–(15.3) associated with the two-dimensional Helmholtz-type equations in the presence of boundary singularities using the SST + MFS approach.

5.1. Examples

In the case of the singular boundary value problems for both the Helmholtz and the modified Helmholtz equations analysed herein, the solution domains under consideration, Ω, accessible boundaries, Γ_{D} and Γ_{N}, and corresponding analytical solutions for $u^{(\mathrm{an})}(\mathbf{x})$ are given as follows:

Example 1. N–D singular problem for the modified Helmholtz equation ($\alpha = 0$ and $\beta = 1$) in a rectangle containing an edge crack OA, see Fig. 1a:

$$\Omega = \mathrm{ABCD} = (-1,1)\times(0,1) \tag{31.1}$$
$$\Gamma_{\mathrm{D}} = \mathrm{AB}\cup\mathrm{CD}\cup\mathrm{DO} = \{-1,1\}\times(0,1)\cup(-1,0)\times\{0\} \tag{31.2}$$
$$\Gamma_{\mathrm{N}} = \mathrm{OA}\cup\mathrm{BC} = (0,1)\times\{0\}\cup(-1,1)\times\{1\} \tag{31.3}$$
$$u^{(\mathrm{an})}(\mathbf{x}) = u_1^{(\mathrm{ND})}(\mathbf{x}) - 1.30\,u_2^{(\mathrm{ND})}(\mathbf{x}) + 1.50\,u_3^{(\mathrm{ND})}(\mathbf{x}) - 1.70\,u_4^{(\mathrm{ND})}(\mathbf{x}), \quad \mathbf{x}\in\overline{\Omega} \tag{31.4}$$

Example 2. D–D singular problem for the modified Helmholtz equation ($\alpha = 0$ and $\beta = 1$) in an L-shaped domain, see Fig. 1b:

$$\Omega = \mathrm{OABCDE} = (-1,1)\times(0,1)\cup(-1,0)\times(-1,0] \tag{32.1}$$
$$\Gamma_{\mathrm{D}} = \mathrm{OA}\cup\mathrm{BC}\cup\mathrm{DE}\cup\mathrm{EO} = (0,1)\times\{0\}\cup(-1,1)\times\{1\}\cup(-1,0)\times\{0\}\cup\{0\}\times(-1,0) \tag{32.2}$$
$$\Gamma_{N} = \mathrm{AB}\cup\mathrm{CD} = \{1\}\times(0,1)\cup\{-1\}\times(-1,1) \tag{32.3}$$
$$u^{(\mathrm{an})}(\mathbf{x}) = u_1^{(\mathrm{DD})}(\mathbf{x}) - 1.30\,u_2^{(\mathrm{DD})}(\mathbf{x}) - 1.70\,u_4^{(\mathrm{DD})}(\mathbf{x}), \quad \mathbf{x}\in\overline{\Omega} \tag{32.4}$$

Example 3. N–N singular problem for the Helmholtz equation ($\alpha = 1$ and $\beta = 0$) in an L-shaped domain, see Fig. 1c:

$$\Omega = \mathrm{OABCDE} = (-1,1)\times(0,1)\cup(-1,0)\times(-1,0] \tag{33.1}$$
$$\Gamma_{\mathrm{D}} = \mathrm{AB}\cup\mathrm{CD} = \{1\}\times(0,1)\cup\{-1\}\times(-1,1) \tag{33.2}$$
$$\Gamma_{N} = \mathrm{OA}\cup\mathrm{BC}\cup\mathrm{DE}\cup\mathrm{EO} = (0,1)\times\{0\}\cup(-1,1)\times\{1\}\cup(-1,0)\times\{0\}\cup\{0\}\times(-1,0) \tag{33.3}$$
$$u^{(\mathrm{an})}(\mathbf{x}) = u_1^{(\mathrm{NN})}(\mathbf{x}) + 1.50\,u_2^{(\mathrm{NN})}(\mathbf{x}) - 0.50\,u_4^{(\mathrm{NN})}(\mathbf{x}), \quad \mathbf{x}\in\overline{\Omega} \tag{33.4}$$

Example 4. D–N singular problem for the Helmholtz equation ($\alpha = 1$ and $\beta = 0$) in a rectangle containing a V-notch with the re-entrant angle $2\omega = \pi/6$, see Fig. 1d:

$$\Omega = \mathrm{OABCD} = (-1,1)\times(0,1)\setminus\Delta\mathrm{ODD}' \tag{34.1}$$
$$\Gamma_{N} = \mathrm{AB}\cup\mathrm{CD}\cup\mathrm{DO} = \{1\}\times(0,1)\cup\{-1\}\times(\sin\omega,1)\cup\{(-\rho,\rho\sin\omega)|0<\rho<1\} \tag{34.2}$$
$$\Gamma_{\mathrm{D}} = \mathrm{OA}\cup\mathrm{BC} = (0,1)\times\{0\}\cup(-1,1)\times\{-1\} \tag{34.3}$$
$$u^{(\mathrm{an})}(\mathbf{x}) = u_2^{(\mathrm{DN})}(\mathbf{x}) - 1.50\,u_3^{(\mathrm{DN})}(\mathbf{x}) + 1.30\,u_4^{(\mathrm{DN})}(\mathbf{x}), \quad \mathbf{x}\in\overline{\Omega} \tag{34.4}$$

It is important to mention that Examples 1–4 have been chosen such that $-k^2$ is not an eigenvalue of the N–D, D–D, N–N and D–N problems, respectively, for the Laplacian in the corresponding domains. All examples analysed in this study contain a singularity at the origin $O(0,0)$ which is caused by the nature of the analytical solutions considered, i.e. the analytical solutions are given as linear combinations of the first four singular functions/eigenfunctions satisfying homogeneous boundary conditions on the edges of the wedge, as well as by a sharp corner in the boundary (Examples 2–4) or by an abrupt change in the boundary conditions at O (Examples 1 and 4), see Fig. 1(a–d).

The singular boundary value problems investigated in this paper have been solved using a uniform distribution of both the boundary collocation points $\mathbf{x}^{\ell}$, $\ell = 1,\ldots,L$, and the source points $\mathbf{y}^{m}$, $m = 1,\ldots,M$, with the mention that the latter were

located on a so-called pseudo-boundary, Γ_S, which has the same shape as the boundary Γ of the solution domain and is situated at the distance $d > 0$ from Γ, see e.g. Tankelevich et al. [50]. In the present computations, the values for the distance d were set to $d = 2$ for Examples 1–3, and $d = 3$ for Example 4. Furthermore, the number of boundary collocation points was set to:

(i) $L = 120$ for Examples 1 and 4, such that $L/3 = 40$ and $L/6 = 20$ collocation points are situated on each of the boundaries BC and OA, AB, CD, DA and OD, respectively;
(ii) $L = 154$ for Examples 2 and 3, such that 19 and 39 collocation points are situated on each of the boundaries OA, AB, DE and EO, and BC and CD, respectively.

In addition, for all examples investigated throughout this study, the number of source points, M, was taken to be equal to that of the boundary collocation points, L, i.e. $M = L$.

5.2. Accuracy errors

In what follows, we denote by $u^{(\mathrm{num})}$ and $q^{(\mathrm{num})}$ the numerical values for the solution and normal flux, respectively, obtained using the least-squares method (LSM), i.e. a direct inversion method, and by subtracting the first $n_S \geqslant 0$ singular functions/eigenfunctions, with the convention that when $n_S = 0$ then the numerical solution and normal flux are obtained using the standard MFS, i.e. without removing the singularity. It should be mentioned that formally the LSM solution, $\tilde{\mathbf{c}}_{LSM}$, of the MFS system of linear algebraic Eqs. (28) is given as the solution of the following normal equation

$$\left(\mathbf{A}^{\mathrm{T}}\mathbf{A}\right)\tilde{\mathbf{c}} = \mathbf{A}^{\mathrm{T}}\mathbf{F}, \tag{35}$$

in the sense that

$$\tilde{\mathbf{c}}_{LSM} = \left(\mathbf{A}^{\mathrm{T}}\mathbf{A}\right)^{-1}\mathbf{A}^{\mathrm{T}}\mathbf{F}. \tag{36}$$

In order to measure the accuracy of the numerical approximation for the solution, $u^{(\mathrm{num})}$, and normal flux, $q^{(\mathrm{num})}$, with respect to their corresponding analytical values, $u^{(\mathrm{an})}$, and, $q^{(\mathrm{an})}$, respectively, we define the *normalized errors*

$$\mathrm{err}(u(\mathbf{x})) = \frac{|u^{(\mathrm{num})}(\mathbf{x}) - u^{(\mathrm{an})}(\mathbf{x})|}{\max_{\mathbf{y}\in\widetilde{\Gamma}}|u^{(\mathrm{an})}(\mathbf{y})|}, \quad \mathrm{err}(q(\mathbf{x})) = \frac{|q^{(\mathrm{num})}(\mathbf{x}) - q^{(\mathrm{an})}(\mathbf{x})|}{\max_{\mathbf{y}\in\widetilde{\Gamma}}|q^{(\mathrm{an})}(\mathbf{y})|}, \tag{37}$$

for the solution and normal flux, respectively, where $\widetilde{\Gamma}$ denotes the set of boundary collocation points, since on using these errors divisions by zero and very high errors at points where the solution and/or normal flux have relatively small values are avoided.

Furthermore, we also introduce an error that measures the inaccuracies in the numerical results obtained for the flux intensity factors, namely the *absolute error* defined by

$$\mathrm{Err}(a_j) = |a_j^{(\mathrm{num})} - a_j|. \tag{38}$$

Here $a_j^{(\mathrm{num})}$ represents the numerical value for the exact flux intensity factor a_j, provided that the latter is available.

5.3. MFS + SST solution for singular problems

The first example investigated contains a singularity at the boundary point O caused by both the abrupt change in the boundary conditions and the nature of the analytical solution, see equation (31.4), in the case of the modified Helmholtz equation. It should be noted that this singularity is of a form which is similar to the case of a sharp re-entrant corner of angle zero, i.e. $\theta_2 - \theta_1 = 2\pi$. This may be seen by extending the domain $\Omega = (-1,1)\times(0,1)$ using symmetry with respect to the x_1-axis, see also Fig. 1a. In this way, a problem is obtained for a square domain containing a crack, namely $\widetilde{\Omega} = (-1,1)\times(-1,1)\setminus[0,1]\times\{0\}$ with zero flux boundary conditions along the crack $[0,1]\times\{0\}$. This problem may also be treated by considering the domain $\widetilde{\Omega}$ described above, with the mention that the singular eigenvectors (11) corresponding to Neumann–Neumann boundary conditions along the crack must be used. However, the original domain Ω and the mixed boundary conditions described in Eqs. (31.2) and (31.3) have been considered in our analysis, i.e. $\theta_2 - \theta_1 = \pi$ as illustrated in Fig. 1a.

Fig. 2a and b present the numerical solution on the boundary $\mathrm{OA} = (0,1)\times\{0\}$ and flux on the boundary $\mathrm{DO} = (-1,0)\times\{0\}$, respectively, obtained for Example 1 when the standard MFS is used, in comparison with their analytical values. From these figures it can be seen that, although the numerical solution represents a good approximation for its analytical counterpart, the boundary flux does not approximate accurately its corresponding analytical value on DO when no singular functions/eigenfunctions are subtracted, i.e. $n_S = 0$, and at the same time having an oscillatory behaviour on this part of the boundary. A similar pattern is observed for the numerical results retrieved for the solution $u|_{\mathrm{DO}}$ and boundary flux $q|_{\mathrm{OA}}$ in the case of the singular problem given by Example 4, as can be seen from Fig. 2c and d, respectively. It should

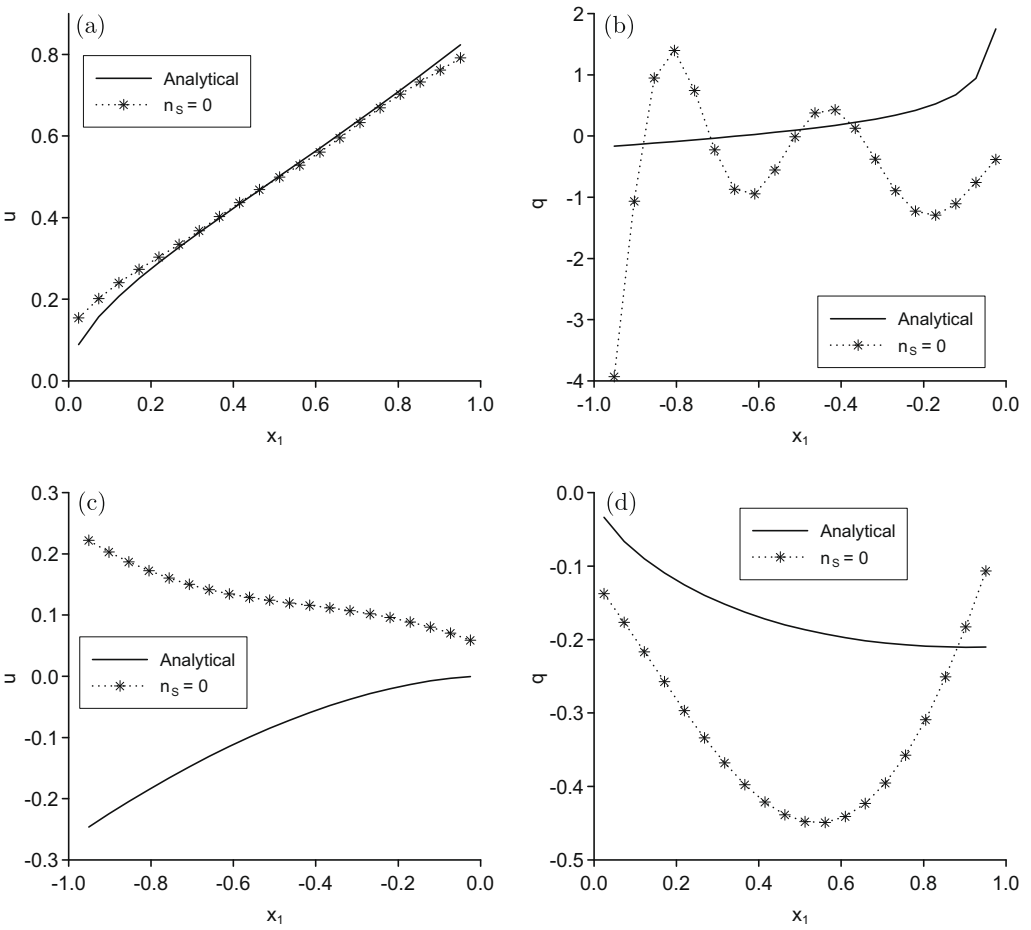

Fig. 2. Analytical and numerical solutions (a) $u|_{OA}$, and (b) $q|_{DO}$, obtained without subtracting any singular functions/eigenfunctions ($n_S = 0$) for the N–D singular problem given by Example 1. Analytical and numerical solutions (c) $u|_{DO}$, and (d) $q|_{OA}$, obtained without subtracting any singular functions/eigenfunctions ($n_S = 0$) for the D–N singular problem given by Example 4.

be mentioned that in this case both the numerical solution and the numerical boundary flux are very inaccurate approximations for their analytical values. Although not presented, it is reported that similar results have been obtained for the singular problems given by Examples 2 and 3, as well as the other unknown boundary solutions and fluxes for all examples investigated.

Fig. 3a and b illustrate a comparison between the analytical and numerical solutions for $u|_{OA}$ and $q|_{DO}$, respectively, obtained by removing various numbers of singular functions/eigenfunctions, namely $n_S \in \{1, 2, 3, 4, 5\}$, for the N–D singular problem given by Example 1. It can be seen from these figures that the numerical results for both the solution and the flux are considerably improved, even if only the first singular function/eigenfunction corresponding to Dirichlet–Neumann boundary conditions on $(-1, 1) \times \{0\}$ is removed, i.e. $n_S = 1$. The same pattern is observed if one continues to remove higher-order singular functions/eigenfunctions in the modified MFS, i.e. $n_S \in \{2, 3\}$, as can be seen from Fig. 3a and b. Moreover, the removal of $n_S \geqslant 4$ singular functions/eigenfunctions from the standard MFS ensures the retrieval of very accurate numerical solutions, which are also exempted from high and unbounded oscillations, for the solution on OA and the flux on DO, respectively, see Fig. 3a and b.

In order to describe quantitatively the influence of the SST over the MFS approach for singular problems associated with two-dimensional Helmholtz-type equations, the normalized errors, $\mathrm{err}(u(\mathbf{x}))$, $\mathbf{x} \in \mathrm{OA}$, and $\mathrm{err}(q(\mathbf{x}))$, $\mathbf{x} \in \mathrm{DO}$, obtained by subtracting various numbers of singular functions/eigenfunctions, namely $n_S \in \{0, 1, 2, 3, 4, 5\}$, for Example 1, are presented on a semi-logarithmic scale in Fig. 3c and d, respectively. From these figures it can be noticed the major effect, in terms of the accuracy, of the modified MFS + SST numerical scheme, namely a significant improvement in the normalized errors for the numerical solution and flux from $O(10^{-2})$ to $O(10^{-8})$ for $\mathrm{err}(u(\mathbf{x}))$, $\mathbf{x} \in \mathrm{OA}$, and from $O(10^{0})$ to $O(10^{-6})$ for $\mathrm{err}(q(\mathbf{x}))$, $\mathbf{x} \in \mathrm{DO}$. As expected, the errors in the numerical flux are larger than those in the numerical solution due to the first-order derivatives occurring in the representation of the flux. Although not presented herein, it is reported that the numerical solution obtained on the remaining boundary of the domain Ω has the same accuracy as that presented on the boundary adjacent to the singular point, thus approximating very accurately the analytical solution.

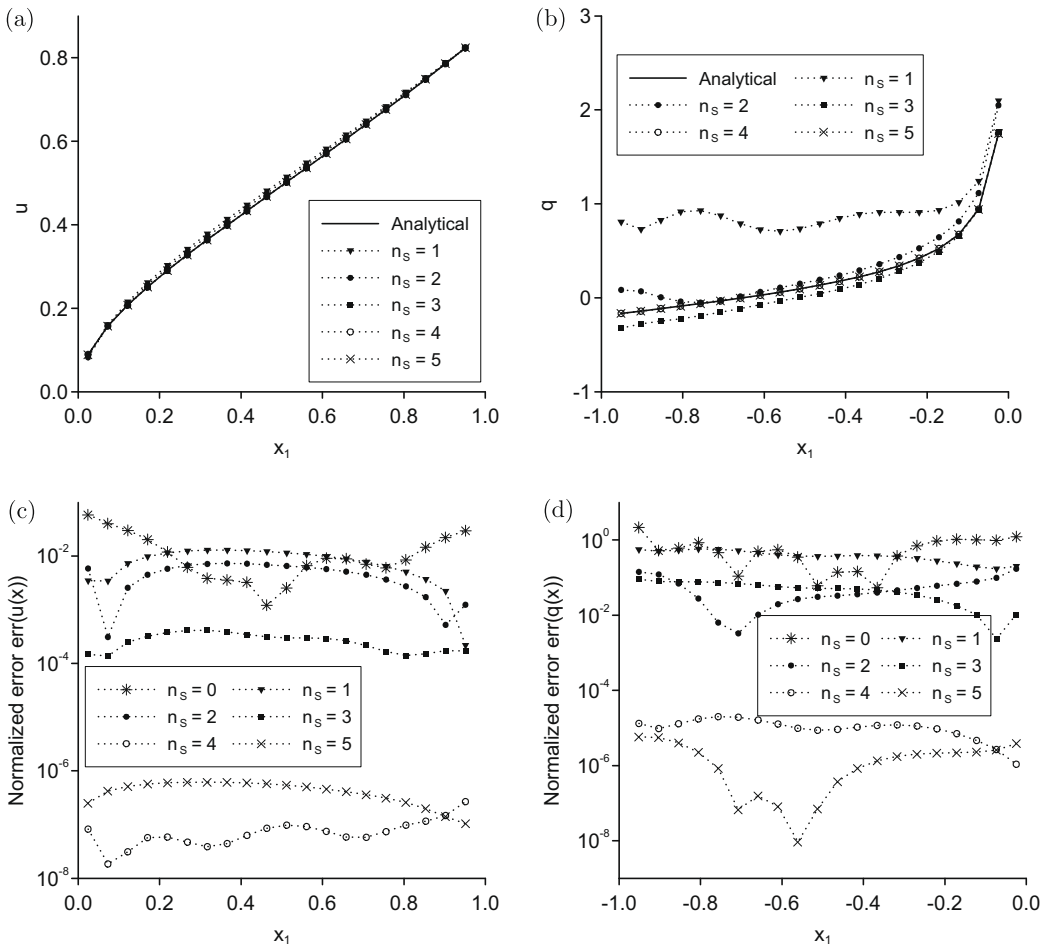

Fig. 3. Analytical and numerical solutions (a) $u|_{OA}$, and (b) $q|_{DO}$, and the corresponding normalized errors (c) $\mathrm{err}(u(\mathbf{x}))$, $\mathbf{x} \in \mathrm{OA}$, and (d) $\mathrm{err}(q(\mathbf{x}))$, $\mathbf{x} \in \mathrm{DO}$, obtained by subtracting various numbers of singular functions/eigenfunctions, namely $n_S \in \{1,2,3,4,5\}$, for the N–D singular problem given by Example 1.

Fig. 4(a–f) show the contour lines for the normalized error $\mathrm{err}(u(\mathbf{x}))$ at internal points $\mathbf{x} \in \Omega_{int} \subset \Omega$ located in a neighbourhood of the singularity point O, namely $\Omega_{int} = (-10^{-2}, 10^{-2}) \times (0, 10^{-2})$, as a function of the number of singular functions/eigenfunctions n_S subtracted from the standard MFS. These figures clearly emphasize the remarkable numerical results obtained also for the solution at internal points situated in the vicinity of the origin, by employing the combined MFS + SST technique. It can be seen form these figures that a significant improvement in the accuracy of the numerical solution takes place, namely from $O(10^0)$ for $n_S = 0$ to $O(10^{-6})$ and $O(10^{-8})$ for $n_S = 4$ and $n_S = 5$, respectively. In the case of Example 1, very accurate numerical results are also obtained for the exact flux intensity factors given by Eq. (31.4), as can be seen from Table 1, which presents the numerical values, $a_j^{(\mathrm{num})}$, for the flux intensity factors, a_j, as well as the corresponding absolute errors defined by Eq. (38).

Both the second and the third examples investigated in this paper contain a singularity at the origin O which is caused by a sharp corner in the boundary, as well as the nature of the analytical solutions corresponding to these problems, i.e. the analytical solutions are given as linear combinations of the first four singular functions satisfying homogeneous Dirichlet or Neumann boundary conditions on the edges of the wedge for Examples 2 and 3, respectively. The analytical and numerical fluxes on the boundaries $\mathrm{EO} = \{0\} \times (-1, 0)$ and $\mathrm{OA} = (0, 1) \times \{0\}$ obtained for Example 2 by subtracting $n_S \in \{1,2,3,4,5\}$ singular functions/eigenfunctions are illustrated in Fig. 5a and b, respectively. Although not presented, it is worth mentioning that the numerical flux obtained on $\mathrm{EO} \cup \mathrm{OA}$ using the standard MFS, i.e. $n_S = 0$, exhibits very high oscillations in the neighbourhood of the singular point and hence it represents an inaccurate approximation for the analytical flux. Even when the first singular function/eigenfunction is subtracted from the MFS, i.e. $n_S = 1$, the numerically retrieved solutions for $q|_{\mathrm{EO}}$ and $q|_{\mathrm{OA}}$ are still oscillatory and inaccurate. Moreover, from Fig. 5a and b it can be seen that also for $n_S = 1$ oscillations in the numerical flux occur even far from the singularity, namely in the vicinity of the points $\mathbf{x} = (0, -1)$ and $\mathbf{x} = (1, 0)$. However, this difficulty can be overcome if instead of the standard MFS, the modified MFS described in the previous section is employed with $n_S \geqslant 2$. From Fig. 5a and b it can be noticed that the accuracy in the numerical flux is slightly improved for $n_S \in \{2,3\}$ and a very good accuracy in the numerical flux on the boundary adjacent to the origin is attained as n_S approaches

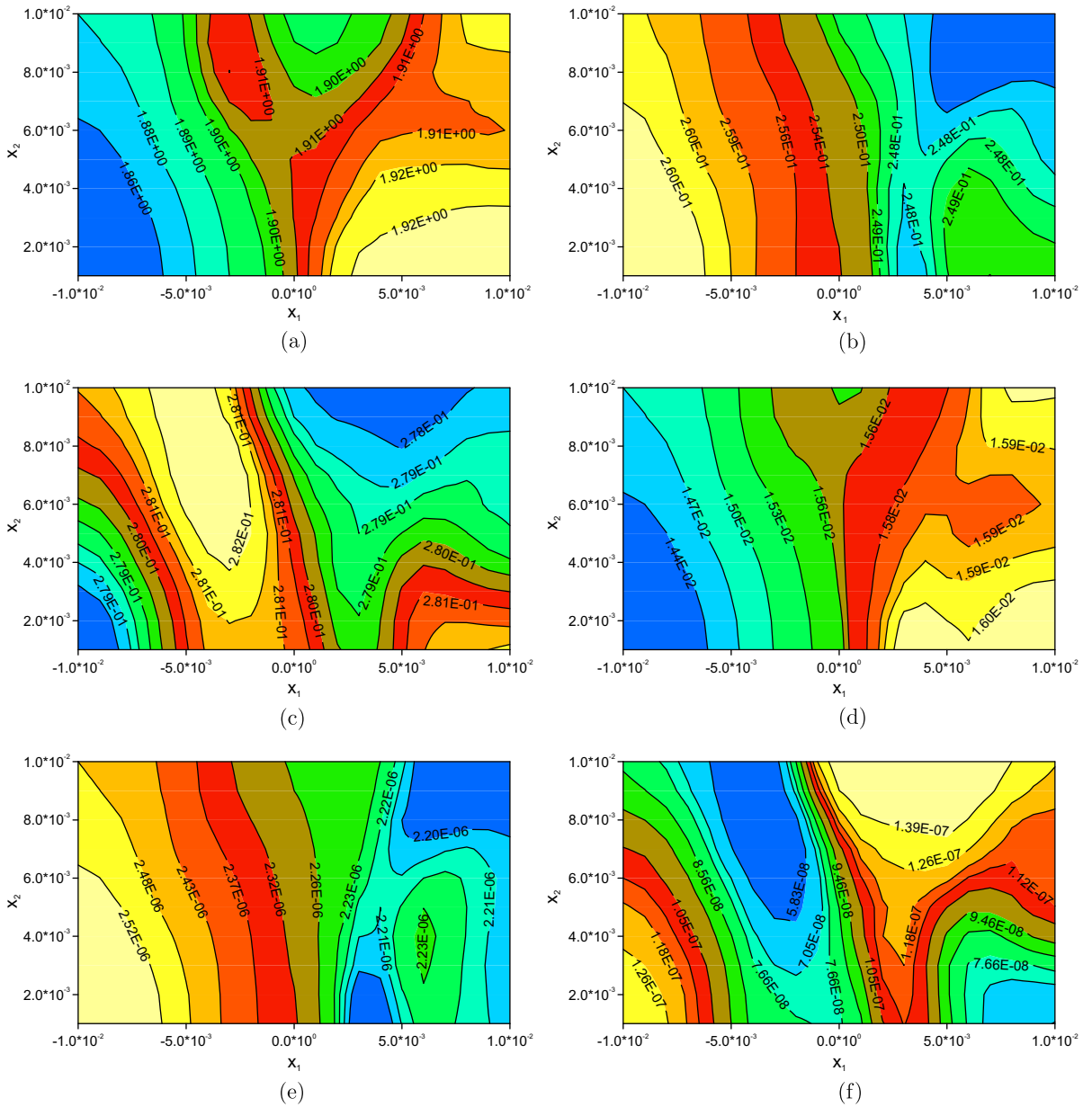

Fig. 4. Contour plot of the normalized error, $\mathrm{err}(u(\mathbf{x}))$, in the neighbourhood, $\Omega_{int} \subset \Omega$, of the singular point O, obtained by subtracting various numbers of singular functions/eigenfunctions, namely (a) $n_S = 0$, (b) $n_S = 1$, (c) $n_S = 2$, (d) $n_S = 3$, (e) $n_S = 4$ and (f) $n_S = 5$, for the N–D singular problem given by Example 1.

Table 1
The numerically retrieved values, $a_j^{(\mathrm{num})}$, $1 \leqslant j \leqslant 4$, for the flux intensity factors and the corresponding absolute errors, $\mathrm{Err}(a_j)$, $1 \leqslant j \leqslant 4$, obtained using the modified MFS and subtracting various numbers of singular functions/eigenfunctions, namely $n_S \in \{1, 2, 3, 4, 5\}$, for the N–D singular problem given by Example 1.

n_S	$a_1^{(\mathrm{num})}$	$\mathrm{Err}(a_1)$	$a_2^{(\mathrm{num})}$	$\mathrm{Err}(a_2)$	$a_3^{(\mathrm{num})}$	$\mathrm{Err}(a_3)$	$a_4^{(\mathrm{num})}$	$\mathrm{Err}(a_4)$
1	1.1538	0.15×10^{0}	–	–	–	–	–	–
2	1.1681	0.16×10^{0}	−1.6624	0.66×10^{0}	–	–	–	–
3	1.0163	0.01×10^{0}	−1.5749	0.27×10^{0}	1.1819	0.31×10^{0}	–	–
4	1.0000	0.10×10^{-7}	−1.3001	0.54×10^{-4}	1.5000	0.30×10^{-4}	−1.6998	0.15×10^{-3}
5	1.0000	0.34×10^{-5}	−1.3000	0.15×10^{-4}	1.4999	0.96×10^{-4}	−1.6994	0.56×10^{-3}

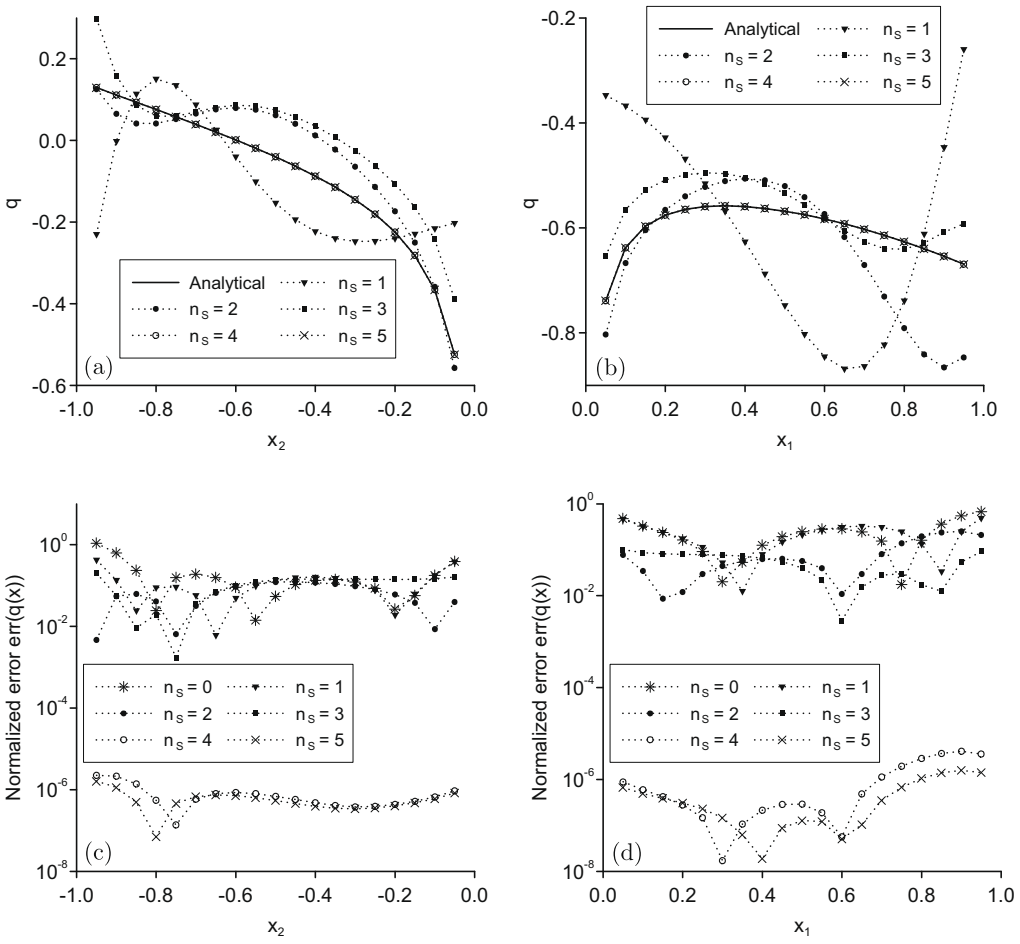

Fig. 5. Analytical and numerical solutions (a) $q|_{EO}$, and (b) $q|_{OA}$, and the corresponding normalized errors (c) $\mathrm{err}(q(\mathbf{x}))$, $\mathbf{x} \in$ EO, and (d) $\mathrm{err}(q(\mathbf{x}))$, $\mathbf{x} \in$ OA, obtained by subtracting various numbers of singular functions/eigenfunctions, namely $n_S \in \{1, 2, 3, 4, 5\}$, for the D–D singular problem given by Example 2.

four, i.e. the number of singular functions satisfying homogeneous Dirichlet boundary conditions on the edges of the wedge used in expression (32.4) for the analytical solution.

Similar conclusions can also be drawn from Fig. 5c and d which present the results shown in Fig. 5a and b in terms of the normalized errors $\mathrm{err}(q(\mathbf{x}))$, $\mathbf{x} \in$ EO, and $\mathrm{err}(q(\mathbf{x}))$, $\mathbf{x} \in$ OA, respectively, as defined by formula (37). Also, from these figures it can be seen the major effect, in terms of accuracy, of the SST applied to the standard MFS, namely a significant improvement in the accuracy of the flux from $O(10^0)$ to $O(10^{-8})$ for $\mathrm{err}(q(\mathbf{x}))$, $\mathbf{x} \in \mathrm{EO} \cup \mathrm{OA}$. The numerical results obtained for the exact flux intensity factors given by Eq. (32.4) are very accurate as the number of singular functions/eigenfunctions, n_S, increases and approaches four and this can be clearly noticed from Table 2, which tabulates the numerical values, $a_j^{(\mathrm{num})}$, for the flux intensity factors, a_j, as well as the corresponding absolute errors for Example 2.

In Example 3 a singular problem in the same L-shaped domain as that considered in Example 2 is analysed, but with Neumman–Neumann boundary conditions on the edges EO and OA adjacent to the singularity point O, for the

Table 2
The numerically retrieved values, $a_j^{(\mathrm{num})}$, $1 \leqslant j \leqslant 4$, for the flux intensity factors and the corresponding absolute errors, $\mathrm{Err}(a_j)$, $1 \leqslant j \leqslant 4$, obtained using the modified MFS and subtracting various numbers of singular functions/eigenfunctions, namely $n_S \in \{1, 2, 3, 4, 5\}$, for the D–D singular problem given by Example 2.

n_S	$a_1^{(\mathrm{num})}$	$\mathrm{Err}(a_1)$	$a_2^{(\mathrm{num})}$	$\mathrm{Err}(a_2)$	$a_3^{(\mathrm{num})}$	$\mathrm{Err}(a_3)$	$a_4^{(\mathrm{num})}$	$\mathrm{Err}(a_4)$
1	0.3374	0.97×10^0	–	–	–	–	–	–
2	1.2299	0.23×10^0	−1.4525	0.15×10^0	–	–	–	–
3	0.8836	0.12×10^0	−1.3265	0.26×10^{-1}	-0.38×10^0	0.38×10^0	–	–
4	1.0000	0.16×10^{-5}	−1.3000	0.12×10^{-6}	0.17×10^{-5}	0.17×10^{-5}	−1.7000	0.85×10^{-6}
5	1.0000	0.12×10^{-5}	−1.3000	0.13×10^{-5}	-0.56×10^{-6}	0.56×10^{-6}	−1.7000	0.17×10^{-5}

two-dimensional Hemholtz equation. Fig. 6a and b show the analytical and numerical solutions on the boundaries EO and OA, respectively, obtained for Example 3 when the modified MFS is used, i.e. $n_S \in \{1,2,3,4,5\}$. Although not presented, it should be mentioned that the numerical solution retrieved without removing the singularities, i.e. $n_S = 0$, is an inaccurate approximation for its corresponding analytical value not only in the vicinity of the singularity point O, but also on the entire edges adjacent to it. This difficulty can also be alleviated by using the MFS in conjunction with the SST. By comparing Fig. 5a and b and Fig. 6a and b, it can be seen that Example 3 is less severe than Example 2, in the sense that, as expected, the knowledge of Dirichlet data on the boundary EO ∪ OA provides more inaccurate numerical results on this portion of the boundary than those obtained by given Neumann data on EO ∪ OA. The same conclusion can be drawn form Fig. 5c and d and Fig. 6c and d which illustrate the numerical results mentioned above in terms of the normalized errors $\mathrm{err}(u(\mathbf{x}))$, $\mathbf{x} \in$ EO, and $\mathrm{err}(u(\mathbf{x}))$, $\mathbf{x} \in$ OA, respectively, for $n_S \in \{0,1,2,3,4,5\}$ singular functions/eigenfunctions subtracted.

Fig. 7(a–f) present the contour lines for the normalized error $\mathrm{err}(u(\mathbf{x}))$ at internal points situated in a neighbourhood of the singularity point O, i.e. $\mathbf{x} \in \Omega_{int} = (-10^{-2}, 10^{-2}) \times (0, 10^{-2}) \cup (-10^{-2}, 0) \times (-10^{-2}, 0]$, as a function of the number, n_S, of singular functions/eigenfunctions subtracted from the standard MFS. These figures clearly illustrate the remarkable numerical results obtained also for the solution at internal points situated in the vicinity of the origin, by employing the combined MFS + SST technique, thus showing a significant improvement in the accuracy of the numerical solution $u(\mathbf{x})$, $\mathbf{x} \in \Omega_{int}$. More precisely, the normalized error $\mathrm{err}(u(\mathbf{x}))$, $\mathbf{x} \in \Omega_{int}$, decreases from $O(10^0)$ for $n_S = 0$ to $O(10^{-7})$ and $O(10^{-8})$ for $n_S = 4$ and $n_S = 5$, respectively. For Example 3, very accurate numerical results are also obtained for the exact flux intensity factors given by Eq. (33.4), as can be seen from Table 3, which presents the numerical values, $a_j^{(\mathrm{num})}$, $1 \leqslant j \leqslant 4$ for the flux intensity factors, a_j, and their corresponding absolute errors $\mathrm{Err}(a_j)$, $1 \leqslant j \leqslant 4$.

Finally, the last example investigated in this paper is the most severe one, in the sense that the singularity at the origin O is caused by the abrupt change in the boundary conditions (i.e. Dirichlet and Neumann boundary conditions on OA and DO, respectively), a sharp corner in the boundary, see Fig. 1d, as well as the nature of the analytical solution, see Eq. (34.4), in the case of the Helmholtz equation. As shown in Fig. 2c and d, both the numerical solution on DO and the numerical boundary

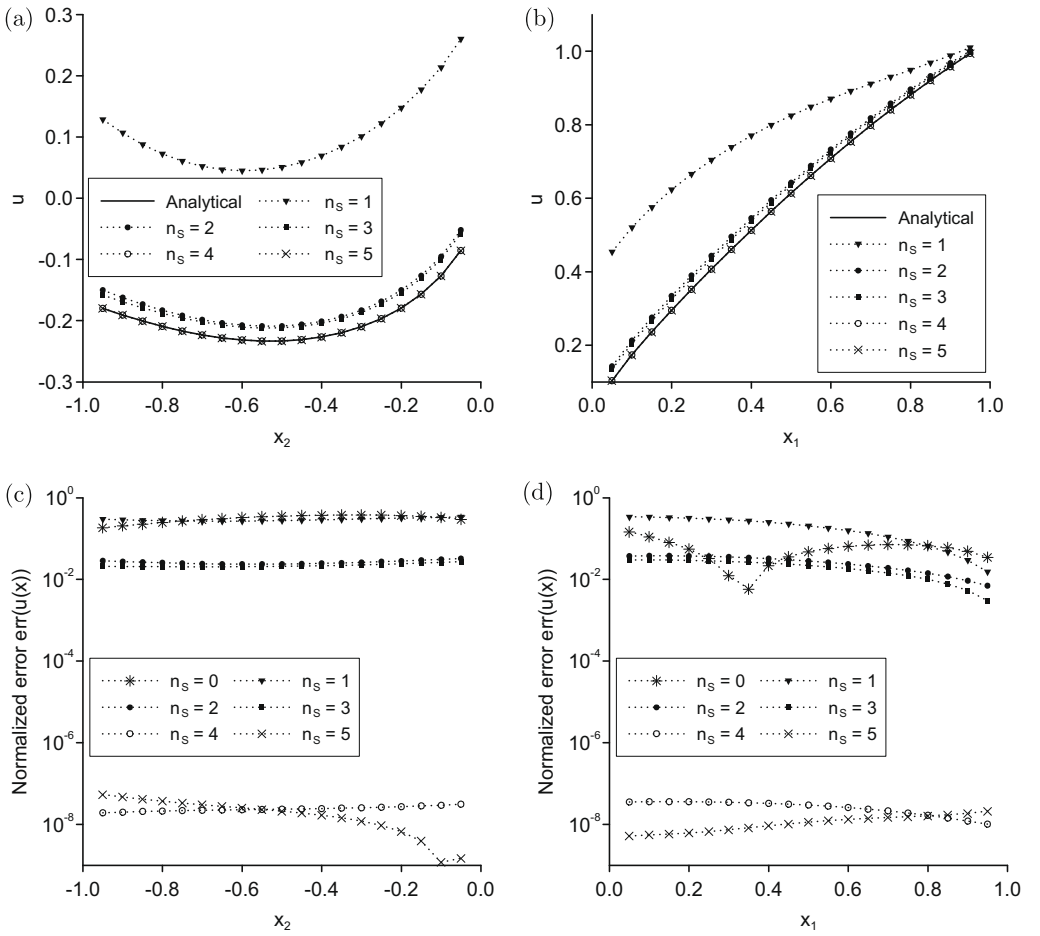

Fig. 6. Analytical and numerical solutions (a) $u|_{\mathrm{EO}}$, and (b) $u|_{\mathrm{OA}}$, and the corresponding normalized errors (c) $\mathrm{err}(u(\mathbf{x}))$, $\mathbf{x} \in$ EO, and (d) $\mathrm{err}(u(\mathbf{x}))$, $\mathbf{x} \in$ OA, obtained by subtracting various numbers of singular functions/eigenfunctions, namely $n_S \in \{1,2,3,4,5\}$, for the N–N singular problem given by Example 3.

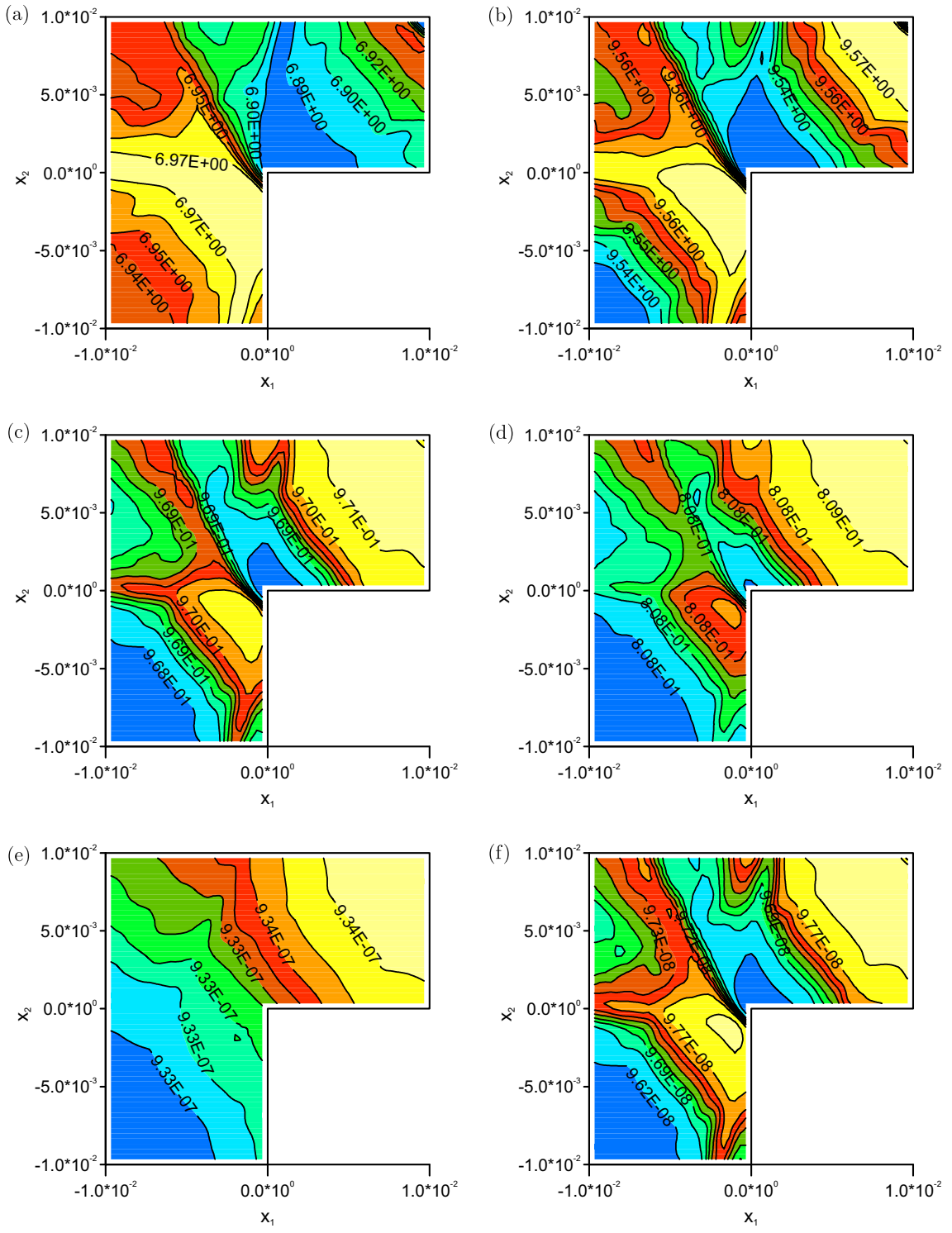

Fig. 7. Contour plot of the normalized error, $\mathrm{err}(u(\mathbf{x}))$, in the neighbourhood, $\Omega_{int} \subset \Omega$, of the singular point O, obtained by subtracting various numbers of singular functions/eigenfunctions, namely (a) $n_S = 0$, (b) $n_S = 1$, (c) $n_S = 2$, (d) $n_S = 3$, (e) $n_S = 4$ and (f) $n_S = 5$, for the N–N singular problem given by Example 3.

flux on OA obtained without removing any singular function/eigenfunction, i.e. $n_S = 0$, represent highly inaccurate approximations for their analytical values. Again, this situation can be overcome by employing the modified MFS presented in Section 4. Consequently, the numerical solution $u^{(\mathrm{num})}|_{\mathrm{DO}}$ and numerical boundary flux $q^{(\mathrm{num})}|_{\mathrm{OA}}$ approach their corresponding

Table 3
The numerically retrieved values, $a_j^{(\mathrm{num})}$, $1 \leqslant j \leqslant 4$, for the flux intensity factors and the corresponding absolute errors, $\mathrm{Err}(a_j)$, $1 \leqslant j \leqslant 4$, obtained using the modified MFS and subtracting various numbers of singular functions/eigenfunctions, namely $n_S \in \{1, 2, 3, 4, 5\}$, for the N–N singular problem given by Example 3.

n_S	$a_1^{(\mathrm{num})}$	$\mathrm{Err}(a_1)$	$a_2^{(\mathrm{num})}$	$\mathrm{Err}(a_2)$	$a_3^{(\mathrm{num})}$	$\mathrm{Err}(a_3)$	$a_4^{(\mathrm{num})}$	$\mathrm{Err}(a_4)$
1	1.0082	0.82×10^{-2}	–	–	–	–	–	–
2	1.0328	0.33×10^{-1}	1.3636	0.14×10^{0}	–	–	–	–
3	1.0150	0.15×10^{-1}	1.4332	0.67×10^{-1}	-0.11×10^{0}	0.11×10^{0}	–	–
4	1.0000	0.24×10^{-7}	1.5000	0.31×10^{-7}	0.12×10^{-6}	0.12×10^{-6}	−0.5000	0.44×10^{-6}
5	1.0000	0.14×10^{-7}	1.5000	0.20×10^{-6}	0.16×10^{-5}	0.16×10^{-5}	−0.5000	0.49×10^{-5}

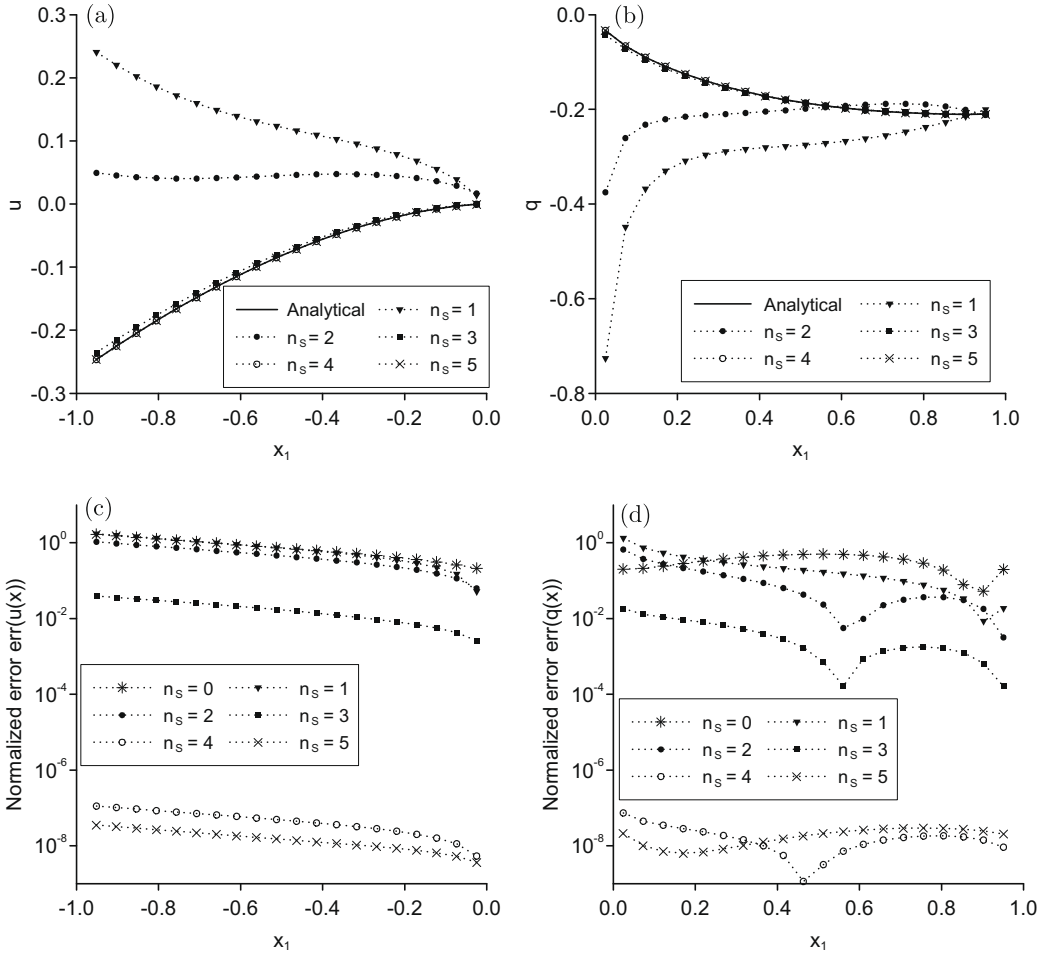

Fig. 8. Analytical and numerical solutions (a) $u|_{\mathrm{DO}}$, and (b) $q|_{\mathrm{OA}}$, and the corresponding normalized errors (c) $\mathrm{err}(u(\mathbf{x}))$, $\mathbf{x} \in \mathrm{DO}$, and (d) $\mathrm{err}(q(\mathbf{x}))$, $\mathbf{x} \in \mathrm{OA}$, obtained by subtracting various numbers of singular functions/eigenfunctions, namely $n_S \in \{1, 2, 3, 4, 5\}$, for the D–N singular problem given by Example 4.

analytical solutions $u^{(\mathrm{an})}|_{\mathrm{DO}}$ and $q^{(\mathrm{an})}|_{\mathrm{OA}}$, respectively, as n_S increases, as can be seen from Fig. 8a and b, with the mention that $n_S \geqslant 4$ ensures very good numerical results for the solution and flux not only far from the singularity, but also in its neighbourhood. These results are also quantitatively presented in Fig. 8c and d which show on a semi-logarithmic scale the corresponding normalized errors $\mathrm{err}(u(\mathbf{x}))$, $\mathbf{x} \in \mathrm{DO}$, and $\mathrm{err}(q(\mathbf{x}))$, $\mathbf{x} \in \mathrm{OA}$, retrieved for various numbers of singular functions/eigenvalues subtracted from the standard MFS, namely $n_S \in \{0, 1, 2, 3, 4, 5\}$. Table 4 presents the absolute errors $\mathrm{Err}(a_j)$, $1 \leqslant j \leqslant 4$, as functions of the number n_S of singular functions removed using the modified MFS, as well as the numerically retrieved flux intensity factors $a_j^{(\mathrm{num})}$, $1 \leqslant j \leqslant 4$. From this table it can be concluded that the numerical flux intensities converge to their exact values as the number n_S of singular functions/eigenfunctions subtracted increases, with the mention that the value $n_S \geqslant 4$ is sufficient in the case of Example 4 for obtaining very accurate numerical estimates for the flux intensity factors.

Table 4
The numerically retrieved values, $a_j^{(\mathrm{num})}$, $1 \leqslant j \leqslant 4$, for the flux intensity factors and the corresponding absolute errors, $\mathrm{Err}(a_j)$, $1 \leqslant j \leqslant 4$, obtained using the modified MFS and subtracting various numbers of singular functions/eigenfunctions, namely $n_S \in \{1,2,3,4,5\}$, for the D–N singular problem given by Example 4.

n_S	$a_1^{(\mathrm{num})}$	$\mathrm{Err}(a_1)$	$a_2^{(\mathrm{num})}$	$\mathrm{Err}(a_2)$	$a_3^{(\mathrm{num})}$	$\mathrm{Err}(a_3)$	$a_4^{(\mathrm{num})}$	$\mathrm{Err}(a_4)$
1	0.32×10^{0}	0.32×10^{0}	–	–	–	–	–	–
2	0.15×10^{0}	0.15×10^{0}	0.6035	0.39×10^{0}	–	–	–	–
3	0.36×10^{-2}	0.36×10^{-2}	1.0476	0.47×10^{-1}	−1.4659	0.34×10^{-1}	–	–
4	-0.20×10^{-7}	0.20×10^{-7}	1.0000	0.15×10^{-8}	−1.5000	0.18×10^{-6}	1.3000	0.11×10^{-5}
5	0.36×10^{-8}	0.36×10^{-8}	1.0000	0.54×10^{-7}	−1.5000	0.22×10^{-7}	1.3000	0.10×10^{-5}

5.4. Convergence of the MFS + SST procedure

If $\widetilde{L}$ MFS collocation points, $\{\mathbf{x}^{(\ell)}\}_{\ell=1}^{\widetilde{L}}$, are considered on the boundary $\widetilde{\Gamma} \subset \Gamma$ then the *root mean square error* (RMS error) on $\widetilde{\Gamma}$ associated with the real valued function $f(\cdot) : \widetilde{\Gamma} \to \mathbb{R}$ is defined by

$$\mathrm{RMS}_{\widetilde{\Gamma}}(f) = \sqrt{\frac{1}{\widetilde{L}} \sum_{\ell=1}^{\widetilde{L}} f(\mathbf{x}^{(\ell)})^2}, \tag{39}$$

In order to investigate the convergence of the algorithm with respect to the distance, d, between the boundary, Γ, and the pseudo-boundary, Γ_S, and the number of singularities, M, we evaluate the following errors corresponding to the solution and

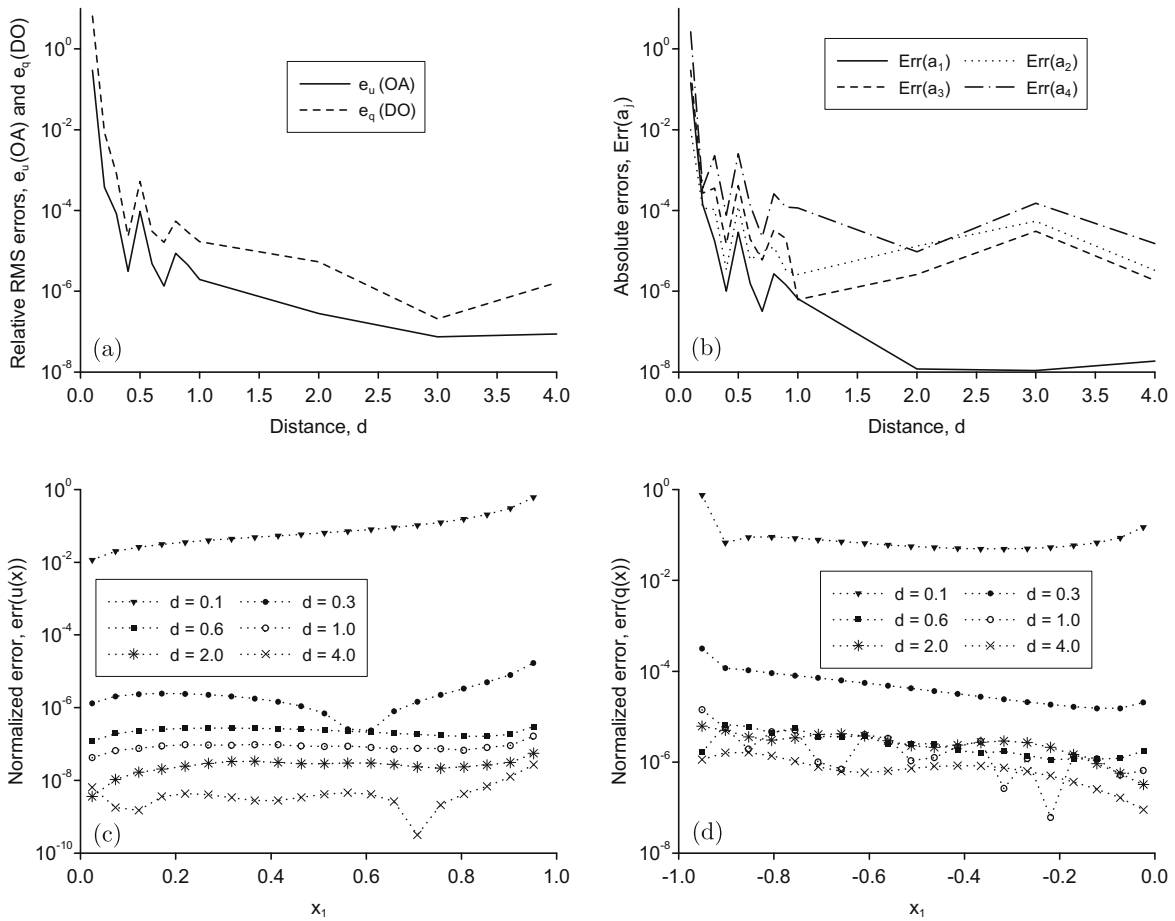

Fig. 9. (a) The relative RMS errors, $e_u(\mathrm{OA})$ and $e_q(\mathrm{DO})$, and (b) the absolute errors, $\mathrm{Err}(a_j)$, $1 \leqslant j \leqslant 4$, as functions of the distance, d, obtained by subtracting $n_S = 4$ singular functions/eigenfunctions for the N–D singular problem given by Example 1. The normalized errors, (c) $\mathrm{err}(u(\mathbf{x}))$, $\mathbf{x} \in \mathrm{OA}$, and (d) $\mathrm{err}(q(\mathbf{x}))$, $\mathbf{x} \in \mathrm{DO}$, obtained by subtracting $n_S = 4$ singular functions/eigenfunctions and using various values of the distance, d, for the N–D singular problem given by Example 1.

flux on each portion of boundary adjacent to the singular point (generically denoted by $\widetilde{\Gamma}$), which are defined as *relative RMS errors*, i.e.

$$e_u(\widetilde{\Gamma}) = \frac{\mathrm{RMS}_{\widetilde{\Gamma}}\left(u^{(\mathrm{num})} - u^{(\mathrm{an})}\right)}{\mathrm{RMS}_{\widetilde{\Gamma}}\left(u^{(\mathrm{an})}\right)}, \qquad e_q(\widetilde{\Gamma}) = \frac{\mathrm{RMS}_{\widetilde{\Gamma}}\left(q^{(\mathrm{num})} - q^{(\mathrm{an})}\right)}{\mathrm{RMS}_{\widetilde{\Gamma}}\left(q^{(\mathrm{an})}\right)}, \tag{40}$$

Fig. 9a shows the relative RMS errors $e_u(\mathrm{OA})$ and $e_q(\mathrm{DO})$, obtained by subtracting $n_S = 4$ singular functions/eigenfunctions, as functions of the distance, d, to the pseudo-boundary where the MFS source points are located, for Example 1. It can be seen from this figure that both errors $e_u(\mathrm{OA})$ and $e_q(\mathrm{DO})$ defined by relation (40) decrease as the distance d increases, with the mention that a very good accuracy of the numerical results is achieved for $d \geqslant 0.3$. Also, as expected $e_u < e_q$ for all $d > 0$, i.e. fluxes are more inaccurate than potential solutions. The same convergent behaviour with respect to increasing the distance between the boundary, Γ, of the solution domain and the pseudo-boundary, Γ_S, is exhibited by the absolute errors, $\mathrm{Err}(a_j)$, $1 \leqslant j \leqslant 4$, and this is presented in Fig. 9b. The convergence of the MFS + SST algorithm with respect to increasing d has also a pointwise character. This feature of the proposed MFS + SST procedure is clearly illustrated in Fig. 9c and d which present the normalized errors $\mathrm{err}(u(\mathbf{x}))$, $\mathbf{x} \in \mathrm{OA}$, and $\mathrm{err}(q(\mathbf{x}))$, $\mathbf{x} \in \mathrm{DO}$, respectively, obtained using $n_S = 4$ and various values of the distance between Γ and Γ_S, namely $d \in \{0.1, 0.3, 0.6, 1.0, 2.0, 4.0\}$, for the N–D singular problem given by Example 1. Similar results have been obtained for the other examples considered in this study and, therefore, they have not presented herein.

Overall, from the examples investigated in this section and the numerical results presented in Figs. 2–9 and Tables 1–4 it can be concluded that the SST applied to the standard MFS is a very suitable method for solving boundary value problems exhibiting singularities caused by the presence of sharp corners in the boundary of the solution domain and/or abrupt changes in the boundary conditions, for both the Helmholtz and the modified Helmholtz equations. The numerical solutions and fluxes retrieved using the MFS + SST technique are very good approximations for their analytical values on the entire boundary, they are exempted from oscillations in the neighbourhood of the singular point and there is no need of further mesh refinement in the vicinity of the singularities. Although not illustrated numerically here, it should be noted that the proposed modified MFS described in Section 4 has provided very accurate results for some other tested cases for two-dimensional Helmholtz-type equations. It should be mentioned, however, that for singular boundary value problems associated with Helmholtz-type equations the numerical results obtained using the proposed MFS + SST procedure are more inaccurate than those retrieved by employing the BEM + SST algorithm introduced by Marin et al. [22].

6. Conclusions

In this study, the MFS was applied for solving accurately and stably problems associated with the two-dimensional Helmholtz-type equations in the presence of boundary singularities. The existence of such boundary singularities affects adversely the accuracy and convergence of standard numerical methods. Consequently, the MFS solutions to such problems and/or their corresponding derivatives, obtained by a direct inversion of the MFS system (i.e. by the LSM or the equivalent normal equation), may have unbounded values in the vicinity of the singularity. This difficulty was overcome by subtracting from the original MFS solution the corresponding singular functions, as given by the asymptotic expansion of the solution near the singularity point. Hence, in addition to the original MFS unknowns, new unknowns were introduced, namely the so-called flux intensity factors. Consequently, the original MFS system was extended by considering a number of additional equations which equals the number of flux intensity factors introduced and specifically imposes the type of singularity analysed in the vicinity of the singularity point. The proposed MFS + SST was implemented and analysed for problems associated with both the Helmholtz and the modified Helmholtz equations in two-dimensional domains containing an edge crack or a V-notch, as well as an L-shaped domain.

From the numerical results presented in this study, we can conclude that the advantages of the proposed method over other methods, such as mesh refinement in the neighbourhood of the singularity, the use of singular BEMs and/or FEMs etc., are the high accuracy which can be obtained even when employing a small number of collocation points and sources, and the simplicity of the computational scheme. A possible drawback of the present method is the difficulty in extending the method to deal with singularities in three-dimensional problems since such an extension is not straightforward.

Acknowledgement

The financial support received from the Romanian Ministry of Education, Research and Innovation through IDEI Programme, Exploratory Research Projects, Grant PN II–ID–PCE–1248/2008, is gratefully acknowledged.

References

[1] T. Apel, A.-M. Sändig, J.R. Whiteman, Graded mesh refinement and error estimates for finite element solution of elliptic boundary value problems in non-smooth domains, Math. Methods Appl. Sci. 19 (1996) 63–85.
[2] T. Apel, S. Nicaise, The finite element method with anisotropic mesh grading for elliptic problems in domains with corners and edges, Math. Methods Appl. Sci. 21 (1998) 519–549.
[3] D.E. Beskos, Boundary element method in dynamic analysis: Part II (1986–1996), ASME Appl. Mech. Rev. 50 (1997) 149–197.

[4] J.T. Chen, M.T. Liang, I.L. Chen, S.W. Chyuan, K.H. Chen, Dual boundary element analysis of wave scattering from singularities, Wave Motion 30 (1999) 367–381.
[5] J.T. Chen, F.C. Wong, Dual formulation of multiple reciprocity method for the acoustic mode of a cavity with a thin partition, J. Sound Vib. 217 (1998) 75–95.
[6] J.T. Chen, J.H. Lin, S.R. Kuo, W. Chyuan, Boundary element analysis for the Helmholtz eigenvalue problems with a multiply connected domain, Proc. R. Soc. London 457 (2001) 2521–2546.
[7] C. Huang, Z. Wu, R.D. Nevels, Edge diffraction in the vicinity of the tip of a composite wedge, IEEE Trans. Geosci. Remote Sensing 31 (1993) 1044–1050.
[8] I. Harari, P.E. Barbone, M. Slavutin, R. Shalom, Boundary infinite elements for the Helmholtz equation in exterior domains, Int. J. Numer. Methods Eng. 41 (1998) 1105–1131.
[9] W.S. Hall, X.Q. Mao, A boundary element investigation of irregular frequencies in electromagnetic scattering, Eng. Anal. Bound. Elem. 16 (1995) 245–252.
[10] P.A. Barbone, J.M. Montgomery, O. Michael, I. Harari, Scattering by a hybrid asymptotic/finite element, Comput. Methods Appl. Mech. Eng. 164 (1998) 141–156.
[11] A.S. Wood, G.E. Tupholme, M.I.H. Bhatti, P.J. Heggs, Steady-state heat transfer through extended plane surfaces, Int. Commun. Heat Mass Transfer 22 (1995) 99–109.
[12] A.D. Kraus, A. Aziz, J. Welty, Extended Surface Heat Transfer, Wiley, New York, 2001.
[13] A.J. Nowak, C.A. Brebbia, Solving Helmholtz equation by boundary elements using multiple reciprocity method, in: G.M. Calomagno, C.A. Brebbia (Eds.), Computer Experiment in Fluid Flow, CMP/Springer Verlag, Berlin, 1989, pp. 265–270.
[14] J.P. Agnantiaris, D. Polyzer, D. Beskos, Three-dimensional structural vibration analysis by the dual reciprocity BEM, Comput. Mech. 21 (1998) 372–381.
[15] J.T. Chen, K.H. Chen, Dual integral formulation for determining the acoustic modes of a two-dimensional cavity with a degenerate boundary, Eng. Anal. Bound. Elem. 21 (1998) 105–116.
[16] B. Schiff, Eigenvalues for ridged and other waveguides containing corners of angle $3\pi/2$ or 2π by the finite element method, IEEE Trans. Microwave Theory Tech. 39 (1991) 1034–1039.
[17] W. Cai, H.C. Lee, H.S. Oh, Coupling of spectral methods and the p-version for the finite element method for elliptic boundary value problems containing singularities, J. Comput. Phys. 108 (1993) 314–326.
[18] T.R. Lucas, H.S. Oh, The method of auxiliary mapping for the finite element solutions of elliptic problems containing singularities, J. Comput. Phys. 108 (1993) 327–342.
[19] X. Wu, H. Han, A finite-element method for Laplace- and Helmholtz-type boundary value problems with singularities, SIAM J. Numer. Anal. 134 (1997) 1037–1050.
[20] Y.S. Xu, H.M. Chen, Higher-order discretised boundary conditions at edges for TE waves, IEEE Proc. Microw. Antennas Propag. 146 (1999) 342–348.
[21] V. Mantič, F. París, J. Berger, Singularities in 2D anisotropic potential problems in multi-material corners, real variable approach, Int. J. Solids Struct. 40 (2003) 5197–5218.
[22] L. Marin, D. Lesnic, V. Mantič, Treatment of singularities in Helmholtz-type equations using the bounadry element method, J. Sound Vib. 278 (2004) 39–62.
[23] Z.-C. Li, T.T. Lu, Singularities and treatments of elliptic boundary value problems, Math. Comput. Model. 31 (2000) 97–145.
[24] V.D. Kupradze, M.A. Aleksidze, The method of functional equations for the approximate solution of certain boundary value problems, USSR Comput. Math. Math. Phys. 4 (1964) 82–126.
[25] R. Mathon, R.L. Johnston, The approximate solution of elliptic boundary value problems by fundamental solutions, SIAM J. Numer. Anal. 14 (1977) 638–650.
[26] G. Fairweather, A. Karageorghis, The method of fundamental solutions for elliptic boundary value problems, Adv. Comput. Math. 9 (1998) 69–95.
[27] M.A. Golberg, C.S. Chen, The method of fundamental solutions for potential, Helmholtz and diffusion problems, in: M.A. Golberg (Ed.), Boundary Integral Methods: Numerical and Mathematical Aspects, WIT Press and Computational Mechanics Publications, Boston, 1999, pp. 105–176.
[28] G. Fairweather, A. Karageorghis, P.A. Martin, The method of fundamental solutions for scattering and radiation problems, Eng. Anal. Bound. Elem. 27 (2003) 759–769.
[29] H.A. Cho, M.A. Golberg, A.S. Muleshkov, X. Li, Trefftz methods for time dependent partial differential equations, CMC: Comput. Materials & Continua 1 (2004) 1–37.
[30] A. Karageorghis, G. Fairweather, The method of fundamental solutions for the numerical solution of the biharmonic equation, J. Comput. Phys. 69 (1987) 434–459.
[31] A. Karageorghis, Modified methods of fundamental solutions for harmonic and biharmonic problems with boundary singularities, Numer. Meth. Part. Diff. Equations 8 (1992) 1–19.
[32] A. Poullikkas, A. Karageorghis, G. Georgiou, Methods of fundamental solutions for harmonic and biharmonic boundary value problems, Comput. Mech. 21 (1998) 416–423.
[33] A. Poullikkas, A. Karageorghis, G. Georgiou, The method of fundamental solutions for inhomogeneous elliptic problems, Comput. Mech. 22 (1998) 100–107.
[34] J.R. Berger, A. Karageorghis, The method of fundamental solutions for heat conduction in layered materials, Int. J. Numer. Methods Eng. 45 (1999) 1681–1694.
[35] J.R. Berger, A. Karageorghis, The method of fundamental solutions for layered elastic materials, Eng. Anal. Bound. Elem. 25 (2001) 877–886.
[36] A. Poullikkas, A. Karageorghis, G. Georgiou, The numerical solution for three-dimensional elastostatics problems, Comput. Struct. 80 (2002) 365–370.
[37] K. Balakrishnan, P.A. Ramachandran, The method of fundamental solutions for linear diffusion-reaction equations, Math. Comput. Model. 31 (2000) 221–237.
[38] A. Karageorghis, G. Fairweather, The method of fundamental solutions for axisymmetric elasticity problems, Comput. Mech. 25 (2000) 524–532.
[39] A. Poullikkas, A. Karageorghis, G. Georgiou, The numerical solution of three-dimensional Signorini problems with the method of fundamental solutions, Eng. Anal. Bound. Elem. 25 (2001) 221–227.
[40] C.J.S. Alves, S.S. Valtchev, Numerical comparison of two meshfree methods for acoustic wave scattering, Eng. Anal. Bound. Elem. 29 (2005) 371–382.
[41] D.L. Young, S.J. Jane, C.M. Fan, K. Murugesan, C.C. Tsai, The method of fundamental solutions for 2D and 3D Stokes problems, J. Comput. Phys. 211 (2006) 1–8.
[42] C.C. Tsai, D.L. Young, C.M. Fan, C.W. Chen, MFS with time-dependent fundamental solutions for unsteady Stokes equations, Eng. Anal. Bound. Elem. 30 (2006) 897–908.
[43] B.T. Johansson, D. Lesnic, A method of fundamental solutions for transient heat conduction, Eng. Anal. Bound. Elem. 32 (2008) 697–703.
[44] M. Katsurada, H. Okamoto, A mathematical study of the charge simulation method, J. Fac. Sci. Univ. Tokyo, Sect. 1A, Math. 35 (1988) 507–518.
[45] M. Katsurada, A mathematical study of the charge simulation method II, J. Fac. Sci. Univ. Tokyo, Sect. 1A, Math. 36 (1989) 135–162.
[46] M. Katsurada, Asymptotic error analysis of the charge simulation method in Jordan region with an analytic boundary, J. Fac. Sci. Univ. Tokyo, Sect. 1A, Math. 37 (1990) 635–657.
[47] M. Katsurada, Charge simulation method using exterior mapping functions, Jpn. J. Ind. Appl. Math. 11 (1994) 47–61.
[48] P.S. Kondepalli, D.J. Shippy, G. Fairweather, Analysis of acoustic scattering in fluids and solids by the method of fundamental solutions, J. Acoust. Soc. Am. 91 (1992) 1844–1854.

[49] M. MacDonell, A Boundary Method Applied to the Modified Helmholtz Equation in Three Dimensions and its Application to a Waste Disposal Problem in the Deep Ocean, MSc Thesis, Department of Computer Science, University of Toronto, 1985.
[50] R. Tankelevich, G. Fairweather, A. Karageorghis, Potential field based geometric modeling using the method of fundamental solutions, Int. J. Numer. Methods Eng. 68 (2006) 1257–1280.